The Plant Cell, Vol. 20: 2696–2713, October 2008, www.plantcell.org

EFD Is an ERF Transcription Factor Involved in the Control of Nodule Number and Differentiation in *Medicago truncatula* [W]

Tatiana Vernié,[a] Sandra Moreau,[a] Françoise de Billy,[a] Julie Plet,[b] Jean-Philippe Combier,[a] Christian Rogers,[c] Giles Oldroyd,[c] Florian Frugier,[b] Andreas Niebel,[a,1] and Pascal Gamas[a,1,2]

[a] Laboratoire des Interactions Plantes Micro-Organismes, Unité Mixte de Recherche, Centre National de la Recherche Scientifique–Institut National de la Recherche Agronomique 2594/441, F- 31320 Castanet Tolosan, France
[b] Institut des Sciences du Végétal, Centre National de la Recherche Scientifique, F-91198 Gif-sur-Yvette, France
[c] Department of Disease and Stress Biology, John Innes Centre, Norwich NR4 7UH, United Kingdom

Mechanisms regulating legume root nodule development are still poorly understood, and very few regulatory genes have been cloned and characterized. Here, we describe *EFD* (for ethylene response factor required for nodule differentiation), a gene that is upregulated during nodulation in *Medicago truncatula*. The EFD transcription factor belongs to the ethylene response factor (ERF) group V, which contains ERN1, 2, and 3, three ERFs involved in Nod factor signaling. The role of EFD in the regulation of nodulation was examined through the characterization of a null deletion mutant (*efd-1*), RNA interference, and overexpression studies. These studies revealed that EFD is a negative regulator of root nodulation and infection by *Rhizobium* and that EFD is required for the formation of functional nitrogen-fixing nodules. EFD appears to be involved in the plant and bacteroid differentiation processes taking place beneath the nodule meristem. We also showed that EFD activated Mt *RR4*, a cytokinin primary response gene that encodes a type-A response regulator. We propose that EFD induction of Mt *RR4* leads to the inhibition of cytokinin signaling, with two consequences: the suppression of new nodule initiation and the activation of differentiation as cells leave the nodule meristem. Our work thus reveals a key regulator linking early and late stages of nodulation and suggests that the regulation of the cytokinin pathway is important both for nodule initiation and development.

INTRODUCTION

Legumes play a crucial role in both ecological and agricultural systems by their capacity to establish a symbiosis with nitrogen-fixing bacteria called rhizobia. This symbiosis involves the formation of a specific organ, the root nodule, which provides the proper microenvironment for nitrogen fixation by bacteroids and nutrient exchange between both partners. The process relies on their mutual recognition via molecular signals and activation of the plant symbiotic program to form rhizobium-infected nodules.

Important progress has been achieved in the past years toward understanding the initial stages of this complex developmental process. Several genes have been identified that play key roles in the perception and transduction of the bacterial Nod factors (NFs), lipo-chito-oligosaccharidic signals essential for triggering the symbiotic genetic program in specific legume hosts (for recent reviews, see Oldroyd and Downie, 2006, 2008; Jones et al., 2007). Three of these genes, *NSP1*, *NSP2*, and *ERN*, encode transcription factors (Oldroyd and Long, 2003; Kalo et al., 2005; Smit et al., 2005; Heckmann et al., 2006; Middleton et al., 2007). Downstream from NF signaling, another putative transcriptional regulator, called NIN, is essential for triggering nodule organogenesis (Schauser et al., 1999; Borisov et al., 2003; Marsh et al., 2007).

The formation of nodule primordia also requires the action of endogenous signals, notably auxin and cytokinins (for reviews, see Ferguson and Mathesius, 2003; Frugier et al., 2008). Indeed, activation by a gain-of-function mutation of a cytokinin receptor (LHK1) is necessary and sufficient to induce spontaneous nodule formation in *Lotus japonicus*, in a process that requires the GRAS domain transcriptional regulator NSP2 (Tirichine et al., 2007). By contrast, loss of function of this cytokinin receptor reduces nodulation both in *Medicago truncatula* and *L. japonicus* (Gonzalez-Rizzo et al., 2006; Murray et al., 2007). Two response regulator genes involved in cytokinin signaling, Mt *RR1* and Mt *RR4*, have also been found to be induced during early stages of nodulation (Gonzalez-Rizzo et al., 2006; Lohar et al., 2006) and are proposed to define a common pathway together with Mt *NIN*, allowing crosstalk between plant cytokinins and bacterial NFs (Gonzalez-Rizzo et al., 2006).

This work on cytokinins has provided some of the first insights into the underlying mechanisms that are responsible for the production of the nodule meristem. In contrast with the NF signaling pathway, only a few genes encoding regulators of nodule development have been identified. The formation of a nodule necessitates the coordination of plant cell and bacterial cell differentiation, leading to nodules containing differentiated bacteroids capable of nitrogen fixation. A Krüppel-like C_2H_2 zinc

[1] These authors contributed equally to this work.
[2] Address correspondence to pascal.gamas@toulouse.inra.fr.
The author responsible for distribution of the materials integral to the findings presented in this article in accordance with policy described in the Instructions for Authors (www.plantcell.org) is: Pascal Gamas (pascal.gamas@toulouse.inra.fr).
[W] Online version contains Web-only data.
www.plantcell.org/cgi/doi/10.1105/tpc.108.059857

finger protein, Mt ZPT2-1, is expressed in vascular tissues of *Sinorhizobium meliloti*–infected roots and nodules and is necessary for the differentiation of bacteroids and of the nitrogen-fixing zone within the nodule (Frugier et al., 2000). A CAAT binding transcription factor, Mt HAP2.1, is necessary for nodule meristem maintenance as well as for bacterial release from infection threads (Combier et al., 2006). The expression of this gene is confined to the nodule meristem, notably because of posttranscriptional controls mediated by the microRNA miR169 (Combier et al., 2006) and differential splicing (Combier et al., 2008).

While these two transcriptional regulators are important for the processes underlying nodule formation, it is clear that many other components will also be necessary. Genetic dissection has revealed a number of loci important for nodule formation, infection thread growth, and bacterial release (Benaben et al., 1995; Schauser et al., 1998; Szczyglowski et al., 1998; Kawaguchi et al., 2002; Kuppusamy et al., 2004; Veereshlingam et al., 2004; Bright et al., 2005; Morandi et al. 2005; Starker et al., 2006; Arrighi et al., 2008; Teillet et al., 2008). However, to date, there are very few loci that have been cloned to reveal the underlying mechanisms inherent to these processes. One exception is *ign* (for *ineffective greenish nodules*), a non-nitrogen fixing and early senescing mutant showing abnormal symbiosome formation. This mutant is affected in a plasma membrane–located ankyrin repeat protein (Kumagai et al., 2007).

Nodulation is a tightly regulated process that ensures appropriate levels of nitrogen fixation to meet the needs of the plant without incurring excessive yield penalties. Autoregulation of nodulation (AON) allows the number of nodules to be systemically controlled by the plant, by signal exchanges between the shoots and the roots (for review, see Oka-Kira and Kawaguchi, 2006). AON involves both the nodule density and the size of the nodulation zone. Mutants defective in AON (called *nts* in *Glycine max*, *har1* in *L. japonicus*, *sunn* in *M. truncatula*, and *sym29* in pea [*Pisum sativum*]; Krusell et al., 2002; Nishimura et al., 2002b; Searle et al., 2003; Schnabel et al., 2005) form five to ten times more nodules than the corresponding wild-type plant, even in the presence of an excess of nitrate, which normally suppresses nodulation. These mutants are affected in a CLAVATA1–like leucine-rich repeat receptor-like kinase, active in the shoots and for which the corresponding ligand(s) remain(s) to be discovered. Nodule number is also regulated by ethylene locally in the root, as the *M. truncatula sickle* (*skl*) mutant is insensitive to ethylene and shows supernodulation (Penmetsa and Cook, 1997), a phenotype also observed in an *L. japonicus* line expressing a mutated ethylene receptor gene (Nukui et al., 2004). Finally, the light-insensitive *L. japonicus astray* mutant, affected in the HY5 bZIP transcription factor, shows a twofold increase in the number of nodules, which appear in a wider zone of the root (Nishimura et al., 2002a).

The ethylene response factor (ERF) family is one of the largest families of plant-specific transcription factors (Nakano et al., 2006), originally named from proteins able to bind the ethylene-responsive element motif (Riechmann and Meyerowitz, 1998). While many ERFs have been associated with plant responses to biotic and abiotic stresses (Gutterson and Reuber, 2004), at least five ERFs have been shown to be involved in the control of organ development, cell division, or differentiation (Wilson et al., 1996; van der Graaff et al., 2000; Banno et al., 2001; Boutilier et al., 2002; Chuck et al., 2002; Kirch et al., 2003; Marsch-Martinez et al., 2006). In addition, one ERF, called ERN (for ERF required for nodulation) has recently been demonstrated to be central for NF signal transduction (Middleton et al., 2007). Indeed, a deletion mutant in the corresponding gene, designated *bit1-1*, is defective in NF induction of early nodulin genes, infection thread development, and nodule meristem establishment. ERN and two other closely related ERFs, designated ERN2 and 3, were also found to bind to the NF-box, a *cis*-element driving NF induction of the early nodulation marker gene Mt *ENOD11*, using a yeast one-hybrid screen (Andriankaja et al., 2007). Finally, an ERF protein distinct from ERNs was also recently shown to be a positive factor of early nodulation stages in *L. japonicus* (Asamizu et al., 2008).

In this article, we report on a symbiotic ERF that we discovered is required for the differentiation of functional Fix^+ nodules, and we call this protein EFD (for ethylene response factor required for nodule differentiation). EFD also seems to participate in an ethylene-independent feedback inhibition of nodulation process and regulates the expression of the primary cytokinin response regulator Mt *RR4.* We therefore propose that the symbiotic roles of EFD may be mediated by Mt *RR4* through a modulation of the cytokinin pathway.

RESULTS

EFD Is an ERF Transcription Factor That Functions in Nodule Development and Regulation

An ERF transcription factor (originally named MtC50408) was initially identified as being upregulated in *M. truncatula* nodules using macroarray analyses (El Yahyaoui et al., 2004) and suppression subtractive hybridization approaches (Godiard et al., 2007). To assess the function of this ERF transcription factor, we used a high-throughput reverse genetic resource available for *M. truncatula* and screened a fast neutron bombardment deletion-TILLING mutant collection using oligonucleotides flanking 2.5 kb from within the promoter region to the end of the coding region. A mutant designated *efd-1* was identified, containing a 1.5 kb deletion covering nucleotides −656 to +915 (Figure 1A), including the TATA box, the start codon, and a large segment of the AP2/ERF domain. This deletion completely abolishes the production of the *EFD* transcript, as verified by quantitative RT-PCR (Q-RT-PCR) analysis (see Supplemental Table 1 online).

The *efd-1* mutant produces more numerous nodules than wild type plants following *S. meliloti* inoculation (about threefold more at 40 d after inoculation [DAI], with plants grown in pouches; statistically significant with $P < 0.001$, Mann and Whitney test) (Figures 1B and 1C). An increase in the nodule number was already detectable at 5 DAI in the *efd-1* mutant (Figure 1D) in the same restricted region as in wild-type roots. This increased nodule density was accompanied by numerous infection threads particularly in the epidermis (Figure 1D), showing wild-type structures. Nodule primordia were more frequently infected by several infection threads in the *efd-1* mutant than in the wild type, leading to broader or multilobed nodules with several meristems

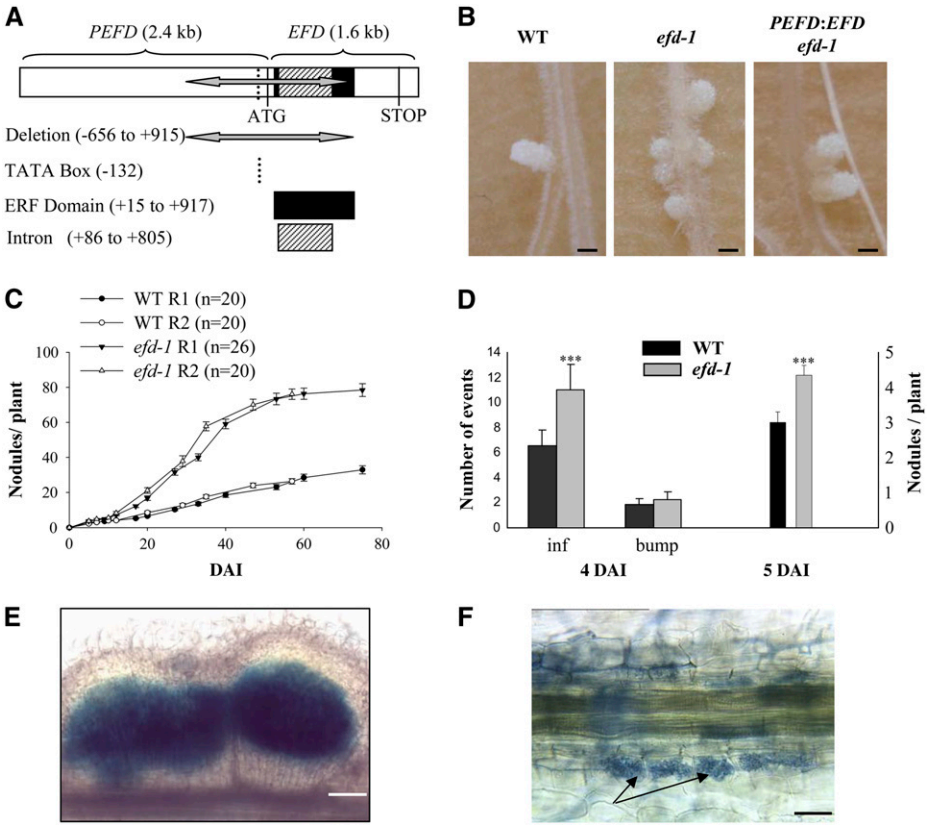

Figure 1. Symbiotic Phenotype of the *efd-1* Mutant.

(A) The *efd-1* deletion encompasses 1571 bp within the promoter (*PEFD*) and the coding region (EFD), including the ERF domain.
(B) Appearance of 27-d-old nodules. From left to right: the wild type (Fix+ and elongated), *efd-1* (Fix$^-$ and more spherical), and *efd-1* complemented by a *PEFD:EFD* construct (Fix+ and elongated). All three samples were collected from the same experiment. Bars = 1 mm.
(C) Time course of *S. meliloti*–induced nodule production in wild-type *M. truncatula* versus the *efd-1* mutant. Two biological repetitions are represented (R1 and R2). Error bars represent SE.
(D) Number of infections, bumps, and nodules counted at 4 DAI (left panel; $n = 10$) or 5 DAI (right panel; $n = 29$) in wild-type *M. truncatula* versus *efd-1*. Statistically significant differences are indicated by asterisks (Mann and Whitney test, $P < 0.001$). Error bars represent SE.
(E) Example of a multilobe nodule (5 DAI) found in the *efd-1* mutant: nonsectioned nodule induced by *S. meliloti hemA-lacZ*, stained in blue following a β-galactosidase assay. Bar = 160 μm.
(F) The *efd-1* mutant exhibits a normal mycorrhization phenotype. Interaction between *M. truncatula* roots and *G. intradices* at 22 DAI. Arrows indicate arbuscules. Bar = 20 μm.

(found in 6 out of 42 *efd-1* nodules at 7 DAI versus none out of 49 wild-type nodules; and in 15 out of 108 *efd-1* nodules versus 3 out of 73 wild-type nodules at 21 DAI) (see an example in Figure 1E).

To examine root nodulation responses at late time points under optimal physiological conditions, we used plants grown under aeroponic conditions (see Methods). A similar difference in the total nodule number was found (on average 46 for *efd-1* versus 26 for wild-type plants at 21 DAI [$n = 9$ roots]). Epidermal and cortical infection threads infections were 5.6- and 2.7-fold more frequent, respectively, in *efd-1* than in wild-type roots. In addition, a striking observation was that cortical cell divisions were much more abundant in the *efd-1* mutant, being frequently associated with early infection structures (versus associated with later stages of infection in wild-type roots). Indeed, they often accompanied root hair curls (58 out of 106 counted curls versus none in wild-type plants; see an example in Supplemental Figure 1 online) and epidermal infection threads (67 out of 104 counted epidermal infections versus 1 out of 18 in wild-type plants). Cortical cell divisions without any associated infection structures were also observed in *efd-1* (on average 7.4 per *efd-1* plant, $n = 9$) but not in wild-type plants.

The second significant feature we noted in *efd-1* nodules was their abnormal development. They were less elongated than wild-type nodules (Figure 1B) and white (therefore defective in leghemoglobin production). They were shown to be defective in nitrogen fixation (Fix$^-$ phenotype) by an acetylene reduction assay (16.2 ± 3.3 [SE] arbitrary units versus nondetectable for wild-type and *efd-1* nodules, respectively). This explained the reduced growth of *efd-1* aerial parts and the chlorotic aspect of

their leaves after 4 weeks in the absence of external combined nitrogen. In the presence of ammonium nitrate, the growth of *efd-1* plants was similar to that of wild-type plants. We also tested the capacity of *efd-1* to undergo symbiotic interactions with the arbuscular mycorrhizal fungus *Glomus intraradices* and found that *efd-1* behaves like wild-type *M. truncatula* (Myc$^+$ phenotype; Figure 1F).

After backcrossing to wild-type *M. truncatula*, we found a strict correlation between an abnormal nodulation phenotype and homozygosity in *efd-1* mutants, which could be distinguished from heterozygous lines by PCR analysis using genomic DNA (125 individuals examined). To confirm that this altered symbiotic behavior resulted from a monogenic recessive mutation in *EFD*, we complemented the mutation in *efd-1* via *Agrobacterium rhizogenes*–mediated root transformation using *EFD* expressed under the control of its own promoter (*PEFD*; 1.0- and 2.4-kb fragments). A normal number of nodules was restored, and elongated nodules similar to the wild type (both visually and by microscopy study) were recovered in 10 (out of 44) plants transformed with *PEFD:EFD* constructs (Figure 1B). In addition, we tested the symbiotic behavior of *M. truncatula* roots transformed with an *EFD* RNA interference (RNAi) construct expressed under the control of the 35S cauliflower mosaic virus promoter. A significant increase in nodulation (Mann and Whitney test, $P < 0.001$) and in the number of infection threads (Mann and Whitney test, $P < 0.05$) was also observed (see Supplemental Figure 2 online) in these roots, corresponding to a weaker *efd* mutant allele.

We can thus conclude that *EFD* participates in the negative regulation of infections and nodule initiations and that it also plays a positive role in the formation of functional Fix$^+$ nodules. By contrast, *EFD* is not involved in mycorrhizal symbiotic interactions.

EFD Overexpression Studies Confirm That EFD Negatively Regulates *S. meliloti* Infections and Nodulation

The role of EFD was further tested by overexpressing *EFD* alone or fused to a VP16 transcriptional activator domain, which allows a transcription factor to be active without any associated cofactors (Wilde et al., 1994). Following *A. rhizogenes*–mediated root transformation, the overexpression of *EFD* in roots was confirmed by Q-RT-PCR with both constructs (12- and 14-fold on average with *P35S:EFD:VP16* and *P35S:EFD*, respectively).

In a nodulation time course, we observed a statistically significant (Mann and Whitney test, $P < 0.001$) threefold reduction in the number of nodules with the *EFD:VP16* construct compared with roots expressing the VP16 domain alone (Figures 2A and 2B), accompanied by a 3.5-fold reduction in the number of infection threads in roots (Figure 2B). A detailed examination of infections showed that the ratio of epidermal versus cortical infection threads was similar in wild-type and EFD-overexpressing roots (see Supplemental Table 2 online). More moderate but qualitatively similar nodulation results were obtained when overexpressing *EFD* without a VP16 fusion (see Supplemental Figure 3 online), suggesting that a protein interacting with EFD within a transcriptional complex might exist.

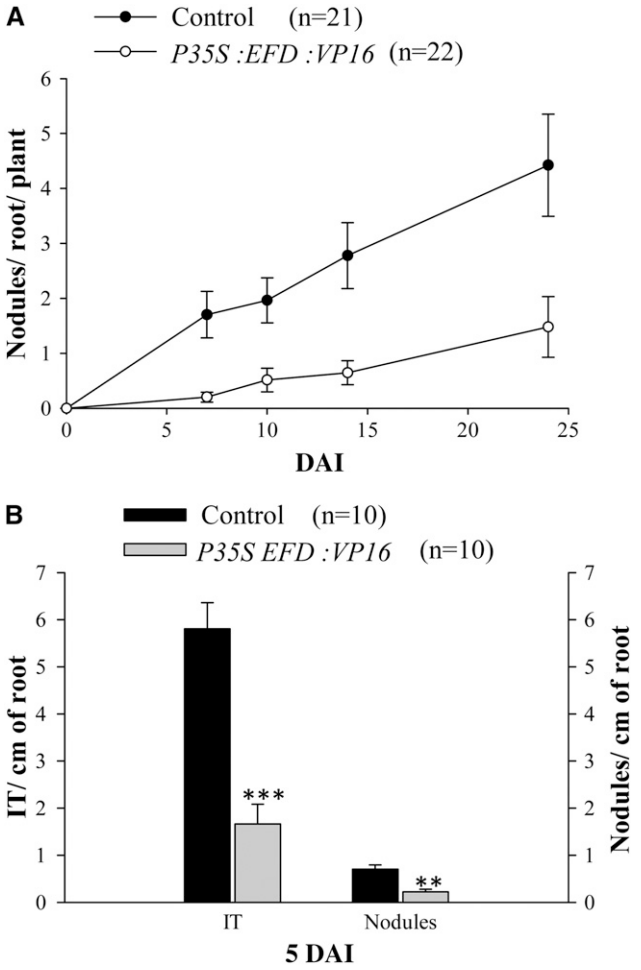

Figure 2. The Number of Infections and Nodules Is Strongly Decreased in Roots Overexpressing *EFD* Fused to the VP16 Activator Domain.

(A) One-month-old transgenic roots expressing *P35S:EFD:VP16* or *P35S:VP16* (Control) constructs were inoculated by wild-type *S. meliloti*. Nodules were counted until 23 DAI. Graphs represent the average of two biological repetitions, and error bars represent SE.

(B) Histograms of infection threads (IT) and nodules number per root at 5 DAI, determined on a third biological repetition. Error bars represent SE. Asterisks indicate statistically significant differences (Mann and Whitney test, $P < 0.001$ [***] and $P < 0.01$[**]).

These results indicate that EFD is a negative regulator of nodulation and *S. meliloti* infections within the root and confirms that the enhanced nodulation phenotype of the *efd-1* mutant is not simply a consequence of a lack of nitrogen fixation.

A Positive Role of EFD in Nodule Differentiation Revealed by Microscopy Observations of the *efd-1* Mutant

To characterize the *efd-1* symbiotic phenotype at the cellular level, we examined nodule sections. At 5 DAI, infection threads were much more numerous and branched in *efd-1* nodules than in wild-type nodules and were found within a region containing

many highly vacuolized cells that were not observed in wild-type nodules (cf. Figures 3A and 3B). Moreover, at this stage, symbiosome formation was observed in the proximal region of wild-type nodules but not of *efd-1* nodules. Indeed symbiosome formation was first observed at 7 DAI in *efd-1*, in much fewer cells than in the wild-type control, with a disorganized distribution of bacteroids (cf. Figures 3C and 3D). At 10 and 20 DAI, *efd-1* nodules showed a wider infection zone II (cf. Figures 3E and 3F) and a strong reduction in the number of infected cells within the zone III (nitrogen-fixing zone in wild-type nodules). Most non-invaded cells of the zone III were crossed by highly branched infection threads, a phenotype not observed in wild-type nodules (cf. Figures 3G and 3H). Amyloplasts were observed in this region, but not in massive amounts, in contrast with some Fix$^-$ mutants (Vasse et al., 1990; Frugier et al., 2000).

The structure of infection threads from wild-type and *efd-1* nodules examined by electron microscopy (EM) studies is shown in Figures 4A and 4B. Infection threads were again observed to be more numerous and branched in *efd-1* nodules, but their wall and matrix were similar to the wild type. Plant cells from nodule zones II and III exhibited an altered cytoplasm in *efd-1*, with a modified endoplasmic reticulum correlated with an accumulation of small vesicles (Figures 4C and 4D). The bacteroid release structures (infection droplets) were often found to be much larger in *efd-1* than in wild-type nodules and present not only in zone II but also in zone III, which was not observed in the wild-type control (Figures 4E and 4F). The size of released bacteroids was normal, but the symbiosome membrane was often more difficult to see. Most bacteroids found in *efd-1* nodules corresponded to the first stages of differentiation (types 1 and 2) (Vasse et al.,

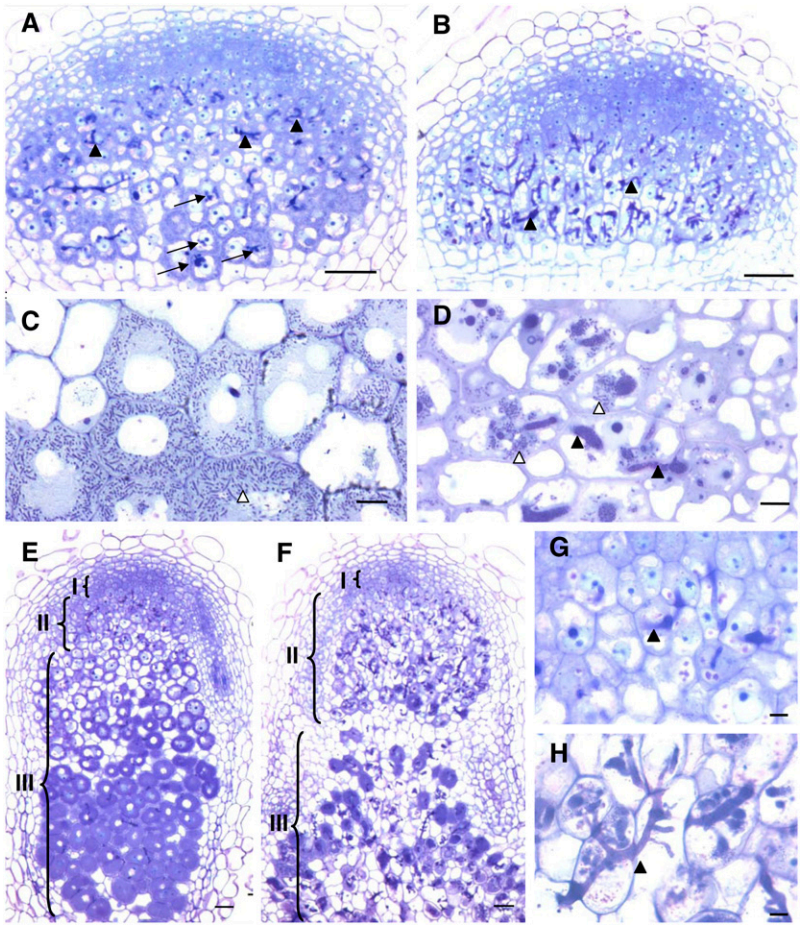

Figure 3. Microscopy Characterization of *efd-1* Nodules Reveals Defects in Symbiosome Formation and Tissue Differentiation.

(A) and **(B)** Four-micrometer sections of 5-d-old nodules, following inclusion in Technovit, induced by *S. meliloti* in wild-type *M. truncatula* **(A)** or the *efd-1* mutant **(B)**. Arrows in **(A)** point to bacterial release in the proximal infection region.

(C) and **(D)** Four-micrometer sections showing infected cells from 7-d-old nodules (zone II) induced by *S. meliloti* in the wild type **(C)** or *efd-1* mutant **(D)** (epon inclusions).

(E) to **(H)** Sections of 10-d-old nodules (Technovit inclusions) induced by *S. meliloti* in the wild type (**[E]** and **[G]**) or *efd-1* mutant (**[F]** and **[H]**). **(G)** and **(H)** are a close-up of the zone II region shown in **(E)** and **(F)**. Black and white arrowheads show infection threads and released bacteria, respectively. Brackets in **(E)** and **(F)** indicate nodule zones I, II, and III. Bars = 10 μm in **(C)**, **(D)**, **(G)**, and **(H)** and 50 μm in **(A)**, **(B)**, **(E)**, and **(F)**.

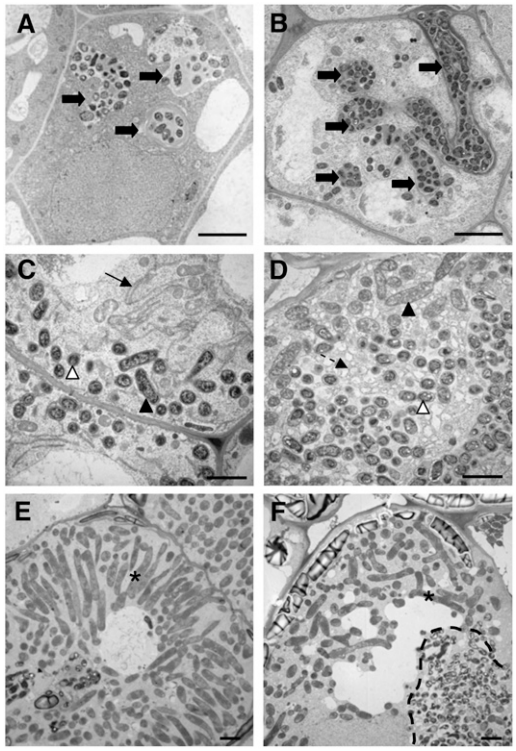

Figure 4. EM Characterization of Zones II and III Cells from Wild-Type *M. truncatula* and *efd-1* 10-d-Old Nodules.

Wild-type nodule (**[A]**, **[C]**, and **[E]**); *efd-1* nodule (**[B]**, **[D]**, and **[F]**).
(A) and **(B)** The arrows show infection threads, which are more numerous and branched in *efd-1* nodules. Bars = 5 μm.
(C) and **(D)** The arrow shows the typical endoplasmic reticulum observed in wild-type nodules, whereas numerous small vesicles are found in *efd-1* nodules (broken arrow). The white and black arrowheads point to bacteroids, types 1 and 2, respectively.
(E) and **(F)** Type 4 bacteroids (asterisks) found in zone III of wild-type nodules and in the proximal region (zone III-like) of *efd-1* nodules; note in *efd-1* the absence of a radial organization of bacteroids, in contrast with wild-type nodules, and the presence of a bacterial release structure (dotted line) next to type 4 bacteroids, generated from an infection thread crossing the cell. Bars = 2 μm in **(C)** to **(F)**.

1990), but a few type 3 and 4 bacteroids were also detected (the type 4 corresponding to the nitrogen-fixing form). These type 4 bacteroids were often Y-shaped and not regularly oriented around a central vacuole as in wild-type zone III cells (Figures 4E and 4F). At 20 DAI, many invaded cells contained degenerating bacteroids, suggesting an early senescence process.

We examined the expression of *S. meliloti nodF*, *bacA*, and *nifH* marker genes, previously used to distinguish bacteroid differentiation stages and to characterize Fix$^-$ mutants (Starker et al., 2006). Indeed, the *nodF* gene, involved in NF synthesis, was shown to be expressed in most Fix$^-$ mutants, in contrast with *bacA* (required for *S. meliloti* survival and differentiation following release from infection threads) and *nifH* (required for nitrogen fixation). Although *nodF* expression was similar in the wild type and in *efd-1* nodules, the abundance of *bacA* transcripts was approximately twofold higher and that of *nifH* transcripts 2.8-fold lower in *efd-1* nodules (see Supplemental Figure 4 online). These results are unlikely to be affected by the number of bacteroids since transcript levels were normalized using the *pnp* gene expression, which is similar in zones II and III (Becker et al., 2004; Naya et al., 2007). This suggests that bacteroids are able to survive in *efd-1* nodules but unable to activate their genetic program responsible for nitrogen fixation.

We thus conclude that EFD is required for the proper development of nodule zones II and III, including symbiosome formation and bacteroid differentiation processes.

EFD Expression Is Found in Nodule Primordia and Nodule Zone II but Is Not Associated with Infection Threads

To further define the role of *EFD* in nodulation, we determined the pattern of *EFD* expression. Q-RT-PCR analysis of various organs of *M. truncatula* revealed that *EFD* is mainly expressed in root nodules, at a higher level in immature nodules (Figure 5A). When we examined *EFD* expression in roots at 1, 2, and 3 DAI with *S. meliloti* (Figure 5B), a 2.3-fold induction compared with non-inoculated roots was observed at 3 DAI ($P < 0.05$, following Cumming et al., 2007). By contrast, purified NF at 10^{-8} M, a concentration at which Mt *ENOD11* is clearly upregulated (Figure 5D), could not activate *EFD* expression in whole roots or isolated root hairs (Figures 5C and 5D). *EFD* was not induced by *S. meliloti* in *M. truncatula* mutants affected in NF perception (*nfp-1*, allele C31) and early signaling (*nsp1-1*, allele B85) (see Supplemental Table 3 online). In contrast with Mt *ENOD11*, no induction of *EFD* was detected in the *hcl-1* mutant (allele B56), which is impaired in nodule development and *S. meliloti* infection, but in which some cortical cell divisions are triggered.

These results suggested that *EFD* expression is not activated during very early stages of the nodulation process. The fact that *EFD* expression is stronger in young than mature nodules also suggested a preferential expression in nodule zone I and/or II, which become relatively less important as the nodule grows. To precisely determine the tissue localization of *EFD* transcripts, we isolated the *EFD* promoter by BAC library screening (see Methods) and generated fusions with the β-glucuronidase (*GUS*) reporter gene. The expression pattern of two promoter segments of 2.4 and 1.0 kb was examined in *A. rhizogenes*–transformed *M. truncatula* roots (Figure 6). Both fusions gave similar results, which were validated by in situ hybridizations performed with a ^{35}S-labeled antisense *EFD* probe. *EFD* expression was found to be distributed in the central region of immature nodules but not in the apical (meristem) region (Figures 6A to 6C) and then confined to the distal part of zone II in differentiated nodules (Figures 6D to 6F). No signal was detected when doing in situ hybridizations with a control sense *EFD* probe (see Supplemental Figure 5 online).

The nodule zone II corresponds to the infection zone, but it also represents the first tissue below the meristem in which plant cell and bacterial differentiation take place. To determine whether *EFD* expression is directly associated with the infection process, we then examined empty nodules induced by an infection-defective *exoA* mutant of *S. meliloti* (Yang et al., 1994). A very clear *PEFD:GUS* expression was detected in 5-d-old *exoA*

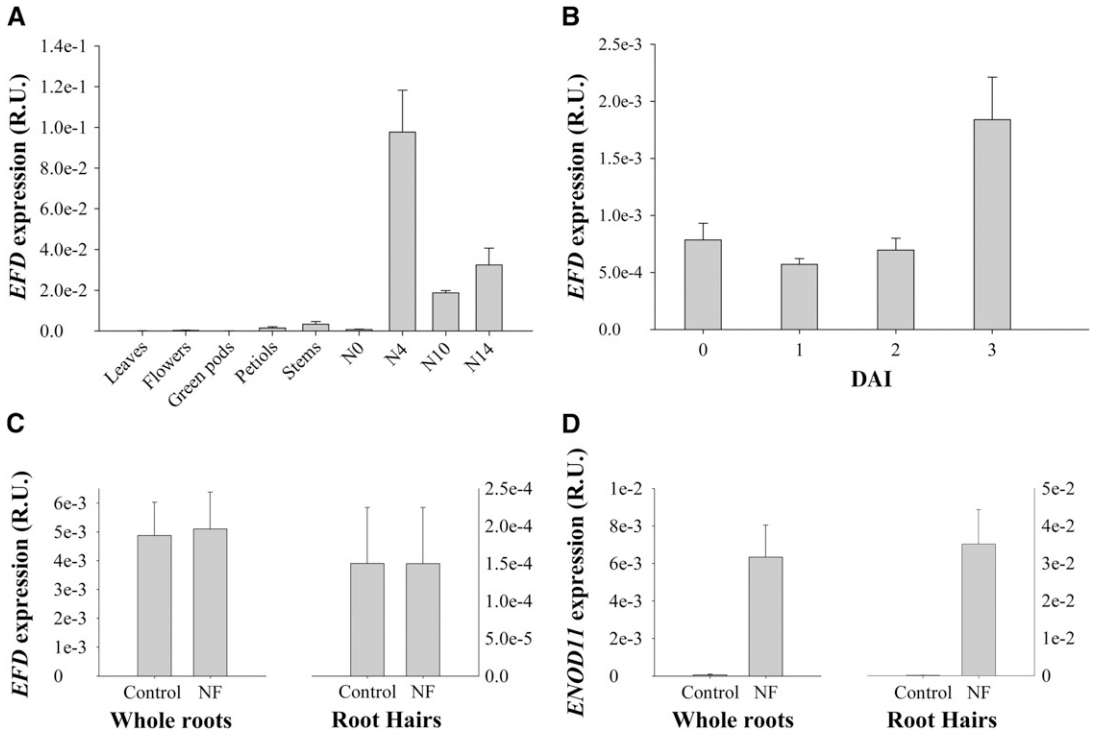

Figure 5. Q-RT-PCR Analyses of *EFD* Expression in Different Tissues.

(A) *EFD* expression in *M. truncatula* leaves, flowers, green pods, petiols, stems, roots (N0), and nodules at different developmental stages (4, 10, and 14 DAI).

(B) *EFD* expression in wild-type *S. meliloti*–inoculated roots of *M. truncatula* at 0, 1, 2, and 3 DAI.

(C) *EFD* expression in NF- or water-treated roots and root hairs (18 h treatment).

(D) Mt *ENOD11* expression in NF- or water-treated roots and root hairs (18 h treatment).

All data are from at least three biological repetitions and are normalized by *EF1-α* expression. Error bars represent SE. R.U., relative units.

nodules (Figure 6G), and this expression disappeared in 10-d-old *exoA* nodules, a stage at which the meristem is no longer active (Figure 6H). This indicated that *EFD* expression in nodules requires an active meristem but is not associated with *S. meliloti* infection per se. This was consistent with the *PEFD:GUS* expression observed at a distance from infection threads in young wild-type nodule primordia (Figure 6I). This expression was first detected at the beginning of nodule primordium formation, associated with cortical cell divisions (Figure 6J). Using these promoter:GUS fusions, we confirmed that NFs did not induce *EFD* expression (see Supplemental Figure 6 online). We also took advantage of these fusions to look for *EFD* expression in non-inoculated roots. We thus found that *PEFD:GUS* was expressed in primary root tips and lateral root primordia (see Supplemental Figure 6 online).

Finally, in view of the reported regulation of some ERFs by ethylene (Guo and Ecker, 2004) and considering the involvement of EFD in the negative regulation of nodulation (Figure 1), we tested the response of *EFD* to this phytohormone. We could not detect any activation of *EFD* expression by 50 μM 1-amino-cyclopropane-1-carboxilate (ACC; ethylene precursor). Moreover, the ethylene inhibitor aminoethoxy-vinyl glycine (AVG) (10 μM) did not change *EFD* activation by *S. meliloti*, and *EFD* was still induced by *S. meliloti* in the ethylene-insensitive *skl* mutant (see Supplemental Figure 7 online).

These results suggest that *EFD* expression is triggered by nodule primordium formation but is not activated during earlier stages of the nodulation process. It then requires meristem activity in nodules.

EFD Is a Member of Group Va of the AP2/EREBP Family

Following Nakano's classification (2006), the *Arabidopsis thaliana* AP2/ERF superfamily, defined as possessing the AP2/ERF domain (59 amino acids), comprises three major families: the ERF family (a single AP2/ERF domain; currently 122 genes, including the DREB protein genes), the AP2 family (two AP2/ERF domains; 18 genes), and the RAV family (one AP2/ERF domain and one B3 domain; six genes). The alignment of the AP2/ERF domain of all *Arabidopsis* ERF proteins reveals seven invariant residues and a set of eight that are found in >95% of the ERF proteins (Nakano et al., 2006). These 15 residues are all found in the AP2/ERF domain of EFD (see Supplemental Figure 8 online). The seven residues involved in direct contact with DNA and the

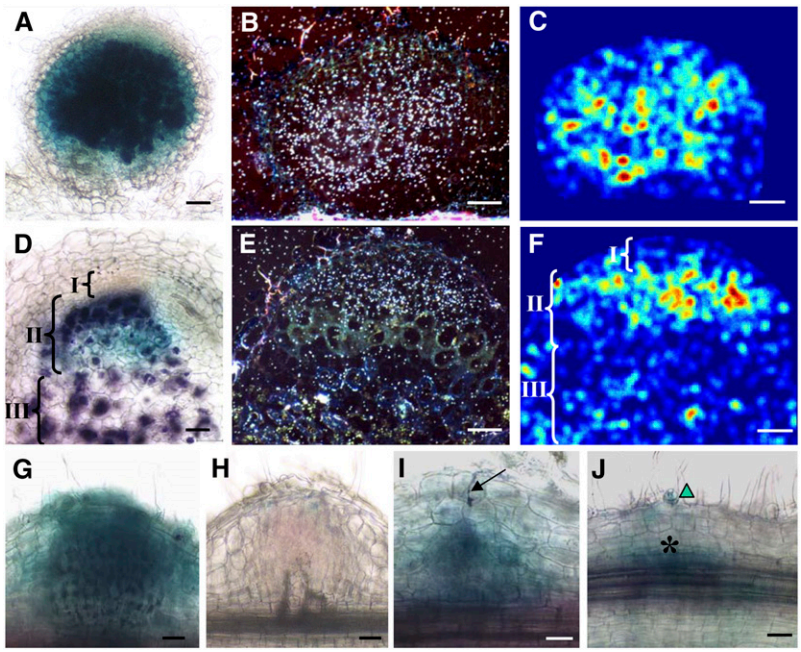

Figure 6. *EFD* Is Expressed in the Apical Zone II of the Nodule and in Nodule Primordia.

(A) to **(F)** Localization of *EFD* mRNA in wild-type 4-d-old (**[A]** to **[C]**) and 10-d-old (**[D]** to **[F]**) nodules, as determined by *PEFD:GUS* fusion (**[A]** and **[D]**; blue) or in situ hybridization (**[B]**, **[C]**, **[E]**, and **[F]**); hybridization signals appear as white dots in **(B)** and **(E)** or false color representation following digitization in **(C)** and **(F)** (Diatrack software) where the strongest signals are indicated by yellow-orange and the weakest by dark-blue colors. *S. meliloti hemA:lacZ* bacteria are stained in purple in **(A)** and **(D)**. Brackets in **(D)** and **(F)** indicate nodule zone I, II and III.

(G) and **(H)** Localization of *EFD* mRNA, based on the *PEFD:GUS* fusion, in 4- and 10-d-old nodules induced by an infection-defective *exoA* mutant of *S. meliloti*.

(I) *PEFD:GUS* expression (blue color) in a wild-type nodule primordium beneath a developing infection thread (arrow) containing *S. meliloti hemA:lacZ* bacteria (purple).

(J) *PEFD:GUS* expression associated with early cortical cell divisions (asterisk) before the elongation of infection threads; note the presence of a curled root hair (triangle), containing *S. meliloti* bacteria (purple).

Bars = 50 μm.

seven Ala residues involved in the stability of the ERF domain (Allen et al., 1998) are also perfectly conserved in EFD, which thus clearly belongs to the AP2/ERF superfamily.

The ERF family has been itself subdivided into 12 groups by a phylogenetic analysis based on the AP2/ERF domains (Nakano et al., 2006). We found that, as the three ERFs involved in NF signaling ERN1, ERN2, and ERN3, EFD belongs to group V (Figure 7). However, EFD is related to a different subgroup (Va) together with *Arabidopsis* ERF#003 (At5g25190, unknown function) and At SHN1, 2, and 3, which regulate the accumulation of epidermal wax (Aharoni et al., 2004). Two differences should be noted within the AP2/ERF domain, concerning two amino acids (a Trp and a Lys residue) directly involved in DNA binding, and which are conserved in the EFD but not in the ERN1-3 subgroup (see Supplemental Figure 8 online).

The analysis of motifs outside the AP2/ERF domain reveals other differences between these ERFs. The ERN1-3 subgroup exhibits CMV-3 and CMV-4 motifs (Nakano et al., 2006; Middleton et al., 2007), whereas the EFD subgroup shares CMV-1 and CMV-2 motifs with unknown function. Finally, *EFD* and At *SHN1*, *2*, *3* genes possess an intron at a conserved position, which is not found in the *ERN1-3* subgroup.

EFD Localizes to the Nucleus

To assess the subcellular location of EFD, fusions were generated at the N and C termini of EFD with the red fluorescent protein (RFP) marker and placed under the control of a 35S promoter. These constructs, as well as a control fusion protein where the AP2/ERF domain was deleted, were transformed into *Nicotiana benthamiana*, and the subcellular protein localization was examined by fluorescence microscopy. Figure 8 shows that the fluorescent signal was exclusively found in the nucleus when using the entire EFD (both for the N- or C-terminal fusion), whereas the deleted fusion protein or the RFP protein alone gave a cytoplasmic signal. This experiment suggests that the EFD AP2/ERF domain plays an important role in targeting EFD to the nucleus.

Possible Targets of the EFD Transcription Factor Revealed by Transcriptome Analyses

As a complementary approach to characterize the *efd-1* phenotype and to look for candidate target genes directly or indirectly controlled by the EFD transcription factor, we performed

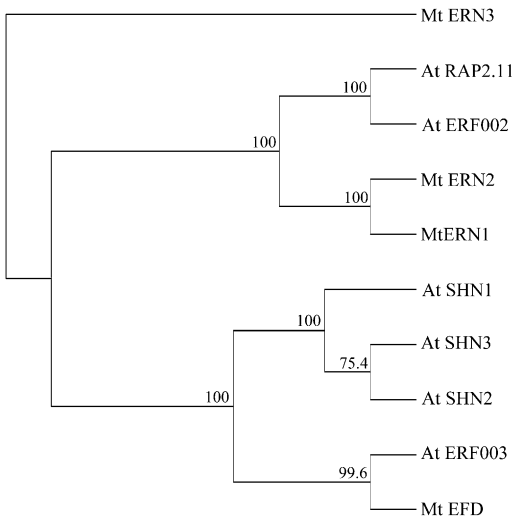

Figure 7. Phylogenetic Tree of Group V ERFs from *Arabidopsis* and *M. truncatula*.

All *Arabidopsis* proteins from ERF group V, as described by Nakano et al. (2006), were aligned with *M. truncatula* group V ERF proteins (ERNs and EFD). Alignment was done with entire proteins. Indicated bootstrap values were determined from 1000 iterations.

microarray analyses, first by comparing *efd-1* and wild-type nodules, at 4 and 10 DAI. We used Mt16KOLI1Plus microarrays representing 16,470 *M. truncatula* EST clusters (Küster et al., 2007). In the following sections, genes are considered as differentially expressed when they show at least a twofold ratio and an adjusted P value ≤ 0.05.

At 4 DAI, no gene was found to be less or more expressed in *efd-1* nodules than in the wild type when taking into account the 0.05 threshold for adjusted P values. By contrast, at 10 DAI, 225 genes were downregulated in *efd-1* compared with wild-type nodules and 34 genes upregulated (see Supplemental Table 4 online). Among the transcripts showing a decreased expression in *efd-1*, several late nodulin genes related to the nitrogen fixation process were found (e.g., encoding leghemoglobins and Gln and Asn synthases), as well as other nodulin genes of unknown function (Mt *N19*, Mt *N20*, and Mt *N31*). By contrast, several early nodulin marker genes were either weakly or not affected (e.g., Mt *ENOD2*, Mt *ENOD16*, and Mt *ENOD40*), while others (e.g., Mt *ENOD11* and Mt *LEC4*) were more expressed in *efd-1* 10-d-old nodules.

A striking observation was the downregulation of a set of 75 *NCR/CCP* (for nodule-specific cysteine-rich/cysteine cluster proteins) genes (Fedorova et al., 2002; Mergaert et al., 2003) and of one *GRP* (glycine-rich protein) gene in *efd-1* 10-d-old nodules. This may be linked to the presumed role of NCRs and GRPs in bacteroid differentiation (Mergaert et al., 2006; Alunni et al., 2007). Among the 34 upregulated genes in *efd-1* 10-d-old nodules, genes coding for peptidases and Cys proteinases were identified, some of which are highly homologous to the SAG2-like senescence-specific genes (Noh and Amasino, 1999), such as As *NODf32*, activated at the onset of nodule senescence (Naito et al., 2000). This is highly reminiscent of Cys proteinases found by cDNA-amplified fragment length polymorphism in the senescent zone IV in *M. truncatula* (Van de Velde et al., 2006). These microarray results were validated by Q-RT-PCR analyses on 48 genes, of which 40 gave qualitatively similar results (see Supplemental Table 5 online).

To look more specifically for genes likely to be regulated by EFD, we used three criteria to be met simultaneously: (1) a reduced expression in *efd-1* nodules versus wild-type nodules at 4 and 10 DAI, (2) an increased expression in *P35S:EFD:VP16* transgenic roots compared with empty vector–transformed roots (microarray analyses; see Supplemental Table 6 online), and (3) an expression profile similar to *EFD* pattern in nodules of wild-type *M. truncatula* induced by various strains of *S. meliloti* (microarray analyses; S. Moreau and P. Gamas, unpublished data). We found only one gene, Mt *RR4*, which clearly met these three criteria among the 34 genes activated in *P35S:EFD:VP16* roots. Q-RT-PCR analyses confirmed that Mt *RR4* expression was strongly decreased in *efd-1* nodules (~16-fold at 4 DAI and sixfold at 10 DAI; see Supplemental Table 5 online) and upregulated in *P35S:EFD:VP16* roots (4.2-fold, using pools of 31 control plants and 54 *EFD*-overexpressing plants). Importantly, in situ hybridizations showed that Mt *RR4* and more generally the type-A response regulator gene family are expressed in nodule zone II, consistent with the *EFD* expression pattern (see Supplemental Figure 9 online). Other nodulin genes expressed in nodule zone II, such as Mt *N6* (Mathis et al., 1999), Mt *ENOD11* (Boisson-Dernier et al., 2005), and Mt *MMPL1* (Combier et al., 2007), were not found to be similarly affected in the *efd-1* and *P35S:EFD:VP16* samples (see Supplemental Table 5 online).

EFD Activates the Expression of Mt *RR4*, a Gene Encoding a Response Regulator That Controls the Cytokinin Signaling Pathway

Mt *RR4* is homologous to *ARR4* from *Arabidopsis*, which encodes a type-A response regulator, induced by cytokinins and

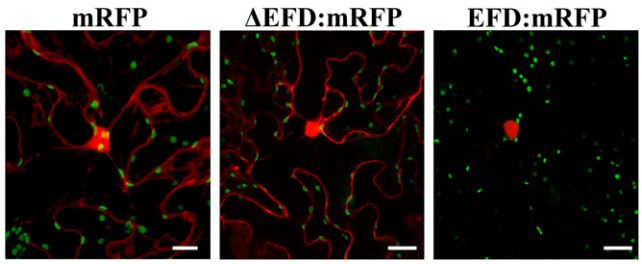

Figure 8. Nuclear Localization of EFD:RFP Fusion Protein.

Leaves of *N. benthamiana* were *A. tumefaciens* transformed with the following constructs, expressed under the control of the 35S promoter: from left to right, reporter mRFP protein alone; mRFP protein fused to a deleted form of EFD lacking the putative DNA binding domain (ΔEFD; N-terminal fusion); full-size EFD fused to mRFP reporter protein (N-terminal fusion). The mRFP reporter protein is detected as a red signal, while green spots correspond to plastids. Note that wild-type EFD is found exclusively in the nucleus in contrast with the mRFP reporter protein alone or to EFD deleted for the ERF domain. Bars = 40 μm.

involved in the negative control of the cytokinin pathway (To et al., 2004). The crucial role of cytokinins in nodulation prompted us to confirm if Mt *RR4* could be transcriptionnally activated by EFD. We first verified that Mt *RR4* is indeed a cytokinin response gene. Using Q-RT-PCR analyses, we observed a 5- to 10-fold transcriptional activation after 1 to 3 h of root treatment with 10^{-7} M benzyl amino purine (BAP) (see Supplemental Figure 10 online). Moreover, this induction took place in the presence of 100 μM cycloheximide, establishing that Mt *RR4* is a primary cytokinin response gene. Using the same samples, we did not find *EFD* to be regulated by BAP (see Supplemental Figure 10 online).

To test a potential role of EFD in the regulation of Mt *RR4* expression, we cotransformed into *N. benthamiana* the *GUS* reporter gene fused to a 1132-bp fragment of Mt *RR4* promoter, along with a *P35S:EFD* construct fused either to a RFP reporter protein or to a HA tag. As a negative control, to detect any possible nonspecific trans-activation effect, we used a Mt *MMPL1* promoter:GUS fusion not controlled by EFD (previous array analyses) and showing a very low basal level of expression in these tissues (Combier et al., 2007). Quantitative analyses of GUS activity in *N. benthamiana* leaf extracts revealed that the Mt *RR4* promoter was clearly activated (on average 8.5-fold on three biological repetitions) by either EFD:RFP (Figures 9A and 9B) or EFD:HA fusions (see Supplemental Figure 11 online). A deletion of the EFD AP2/ERF domain abolished this trans-activation. Similar experiments performed with ERN1, 2, and 3 (ERFs involved in NF signaling) did not reveal any trans-activation of Mt *RR4* (F. de Carvalho Niebel, personal communication). Finally, we also tested whether EFD is able to regulate its own expression and found that EFD was indeed able to trans-activate its own promoter (on average sixfold on three biological repetitions; Figures 9A and 9B), suggesting a positive feedback loop for EFD.

We can thus conclude that the expression of the primary cytokinin response gene Mt *RR4* and of the *EFD* gene itself is directly or indirectly controlled by EFD.

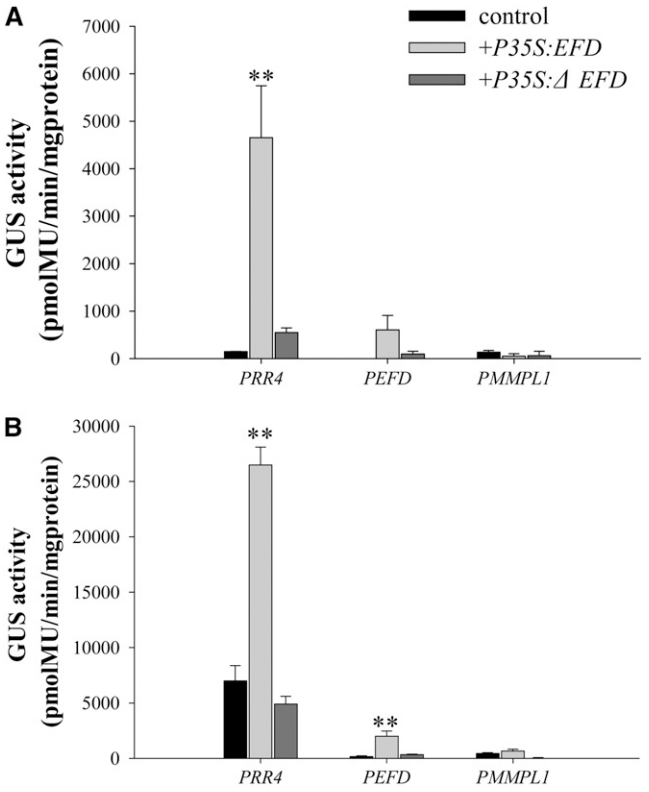

Figure 9. Trans-Activation of *PRR4*, *PEFD*, and *PMMPL1* in *N. benthamiana*.

(A) GUS activity at 24 h following cotransformation.
(B) GUS activity at 48 h following cotransformation.
For both **(A)** and **(B)**, leaves of *N. benthamiana* were cotransformed by *A. tumefaciens* with *PRR4:GUS*, *PEFD:GUS*, or *PMMPL1:GUS* plus either *P35S:EFD:RFP* or *P35S:ΔEFD:RFP* (ΔEFD is EFD deleted for its putative DNA binding domain). Controls correspond to leaves of *N. benthamiana* transformed with *PRR4:GUS*, *PEFD:GUS*, or *PMMPL1:GUS* alone. GUS activity was measured using 10 μg of total protein extracts at 24 **(A)** and 48 **(B)** h after transformation using three biological repetitions. Error bars represent SE. *PRR4* was only significantly activated by EFD at 24 and 48 H and *PEFD* at 48H ($P < 0.01$ for both, following Cumming et al., 2007). *PMMPL1* was not significantly activated.

DISCUSSION

We have identified a transcription factor involved in the rhizobium-legume symbiotic interaction, EFD, that belongs to the large AP2/ERF family. A null mutant of *EFD* is severely affected in its capacity to differentiate functional Fix^+ nodules and shows increased number of nodules compared with a wild-type line. These experiments coupled with RNAi and overexpression approaches support a role of EFD both in the regulation of nodule number and nodule differentiation. Transcriptomic studies and trans-activation assays allowed us to demonstrate that Mt *RR4*, encoding a type-A response regulator of cytokinin signaling, is a target of EFD in *S. meliloti* infected roots and nodules. We propose that EFD may regulate diverse symbiotic responses through interaction with cytokinin signaling.

EFD, a New ERF Transcription Factor Linked to Symbiosis

EFD is different in terms of sequence from the three previously described *M. truncatula* ERFs involved in rhizobium-legume symbiotic interactions (ERN1, 2, 3; Andriankaja et al., 2007; Middleton et al., 2007), even though they belong to the same ERF group (group V). It is therefore expected that different target genes are controlled by EFD and ERN transcription factors. Indeed, ERN1, 2, and 3 bind to the promoter of the early nodulin gene Mt *ENOD11* (Andriankaja et al., 2007), whereas there is no indication that this is the case for EFD. Conversely, the response regulator gene Mt *RR4* appears to be controlled by EFD, but not by ERN proteins (F. de Carvalho Niebel, personal communication).

Another important difference between *EFD* and *ERN* genes is their expression pattern. The three *ERN* genes are constitutively expressed in root hairs, upregulated by NF treatment, and moderately regulated (up or down) in nodules (Andriankaja et al., 2007; Middleton et al., 2007). By contrast, *EFD* expression is not detected in root hairs, is not induced by NF treatment (up to 48 h), and is strongly activated in nodule primordia and infection

zone II. The *EFD*-inducing signal during symbiosis is likely not ethylene as *EFD* is not induced by an ACC treatment and is still induced by *S. meliloti* in the ethylene-insensitive *skl* mutant. The nature of this signal remains to be identified.

EFD is also different from Lj ERF1 (Asamizu et al., 2008), considering different criteria: Lj ERF1 belongs to a distinct ERF group (group IX in the classification of Nakano et al., 2006); Lj *ERF1* is upregulated much earlier and only in root epidermis following *Mesorhizobium loti* inoculation (without any expression in nodules); Lj *ERF1* seems to be a positive regulator of early nodulation processes, based notably on RNAi and overexpression experiments (Asamizu et al., 2008).

EFD Is a Negative Regulator of Nodule Initiation and Is Required for Late Stages of Nodule Development

Two distinct symbiotic phenotypes, early and late, have been revealed by the characterization of the *efd-1* knockout mutant, RNAi studies, and overexpression of activated EFD. The early phenotype is a significant increase in the knockout and knockdown lines in the number of *S. meliloti* infections and nodules compared with wild-type *M. truncatula.* This increase is detected well before the onset of nitrogen fixation in wild-type lines, ruling out at this stage an indirect effect linked to the defect in nitrogen fixation, observed in other Fix$^-$ mutants, such as the *sst1-2 L. japonicus* mutant defective in a sulfate transporter (Krusell et al., 2005). This opens the possibility that EFD participates in the negative regulation of nodulation, together with other (e.g., ethylene-dependent) mechanisms. Our observations suggest that the *efd-1* mutation first leads to local effects on nodule density. Further experiments will be required to determine whether *EFD* may also exert a systemic effect, as in AON (Oka-Kira and Kawaguchi, 2006).

The *EFD*-dependent regulation may be triggered by nodule primordium formation and related to the early *EFD* expression detected in these primordia. We showed that this regulation clearly influences the number of epidermal infections, even though *EFD* is not expressed in close proximity to infection threads or in root hairs. This represented the earliest difference that we detected in the symbiotic behavior between *efd-1* and wild-type plants (or *EFD*-overexpressing and wild-type roots) and might thus be considered as the primary effect of *EFD*-dependent regulation. However *S. meliloti*–inoculated *efd-1* roots also showed an excess of cortical cell divisions compared with wild-type plants, accompanying root hair curls and epidermal infection threads or without associated visible infection structures in some cases. Overall, *efd-1* cortical cells thus seem more reactive to *S. meliloti* infections, which would represent an attractive hypothesis regarding a possible involvement of the cytokinin pathway (see below). However, an alternative hypothesis could be that the slowing down of infection thread development in *efd-1* at late stages would lead to an altered coordination between infections and cortical cell divisions.

The second altered symbiotic phenotype of *efd-1* is the production of Fix$^-$ nodules, in which fewer bacteroids differentiate, as shown both by EM studies and a reduced expression of the *S. meliloti nifH* marker gene. An increased accumulation of *S. meliloti bacA* transcripts is also observed, which may be related to an enlarged nodule zone II. The rare type 4 bacteroids observed are not found in regular rays well organized around a central vacuole as in wild-type nodule zone III (Timmers et al., 1999). Previous work has established that the bacteroid organization in wild-type zone III is linked to the microtubular cytoskeleton (Timmers et al., 1999), which is thus likely to be altered in *efd-1* nodules.

It can thus be proposed that *EFD* plays a positive role in both bacterial and plant cell differentiation. Transcriptomic comparison of *efd-1* and wild-type nodules showed that differences are moderate in 4-d-old nodules but strong in 10-d-old nodules, supporting a role of *EFD* in late stages of nodule development. Whereas the expression of early nodulin genes is not affected (Mt *ENOD2* or Mt *ENOD40*) or even increased (Mt *ENOD11*, a zone II gene) in 10-d-old *efd-1* nodules, nodulin genes associated with the nitrogen fixation process are poorly expressed, consistently with the Fix$^-$ phenotype. A striking observation is the downregulation in *efd-1* nodules of numerous *NCR/CCP* genes that belong to the large family encoding Cys-rich peptides specifically found in indeterminate nodules of hologalegoid legumes (Fedorova et al., 2002; Mergaert et al., 2003; Graham et al., 2004; Silverstein et al., 2006, 2007; Alunni et al., 2007). These peptides are similar to defensins and have been proposed to be involved in bacteroid differentiation by acting as antimicrobial peptides (Mergaert et al., 2006). The downregulation of 75 NCR genes in *efd-1* correlates with the bacteroid differentiation defects detected by microscopy. In addition, six plant genes related to senescence are upregulated in 10-d-old *efd-1* nodules. An early senescence process is thus likely to take place in *efd-1* nodules, which may explain the disappearance of the endoplasmic reticulum correlated with the appearance of numerous small vesicles observed in our EM studies. The fact that *bacA* transcripts are abundant in *efd-1* nodules indicates, however, that *S. meliloti* bacteria survive after release from infection threads (Glazebrook et al., 1993), which is confirmed by our EM studies. We thus favor the hypothesis that this early senescence process is a consequence of defects in plant and/or bacteria differentiation. However, we cannot exclude, with our data, the converse hypothesis that differentiation defects result from early nodule senescence.

To our knowledge, the *efd-1* mutant does not strictly resemble any of the already described Fix$^-$ *M. truncatula* mutants. Nevertheless, it can be noted that abnormal proliferation of infection threads has also been reported for *nip* (Veereshlingam et al., 2004), *sym1* (TE7) (Benaben et al., 1995), and RNAi *DMI2* lines (Limpens et al., 2005). Defects in bacterial release and/or bacteroid differentiation have also been observed for *sym1*, RNAi *DMI2*, and antisense Mt *Zpt2-1* lines (Frugier et al., 2000). However, other features of these mutants differ from *efd-1*, such as a strong defense response and an early stop in nodule development observed in *nip*, normal nodule elongation in *sym1*, and strong accumulation of amyloplasts in nodules of antisense Mt *zpt2-1* lines. The *efd-1* mutant may resemble class 3 *dnf* mutants, as defined by Starker et al. (2006), but plant gene expression and nodule structure (Pislariu and Dickstein, 2007) seem to be differently affected in *efd-1* than in *dnf4* and *dnf7*.

So far, Mt ZPT2-1 and EFD represent the only two transcription factors known to participate in the coordinated differentiation

process of the plant and bacterial partners taking place during late stages of nodule development.

EFD Activates a Type-A Response Regulator Gene

To explore how EFD could act during nodulation, we searched for target genes by comparing transcriptomes of wild-type and *efd-1* nodules as well as *EFD*-overexpressing roots. Expression of the best candidate target gene, Mt *RR4*, was trans-activated in *N. benthamiana* by a *P*35S:*EFD* construct. However, such experiments do not indicate whether EFD binds directly Mt *RR4* promoter.

Mt *RR4* is highly similar to type-A response regulator genes, demonstrated to be primary response genes to cytokinins in *Arabidopsis* (for review, see Ferreira and Kieber, 2005). We confirmed that Mt *RR4* is itself rapidly induced by exogenous cytokinin in a process that does not require de novo protein synthesis. Since type-A response regulator genes are thought to negatively control the cytokinin pathway (for reviews, see Ferreira and Kieber, 2005; Doerner, 2007), itself required for nodulation (Lohar et al., 2004; Gonzalez-Rizzo et al., 2006; Frugier et al., 2008), the activation of Mt *RR4* by EFD provides a possible mechanism regarding the early negative role of EFD on regulation of nodule number. Hence, EFD activation at around 3 DAI may restrict cytokinin signaling and function to prevent further rhizobial infections and nodule initiation. Conversely, as mentioned above, one explanation for the increased abundance of cortical cell divisions in the *efd-1* mutant could be an overactivation of the cytokinin pathway. Further experiments will be needed to test these hypotheses.

The role of cytokinins at later stages of nodule development is still poorly documented. Reporter gene fusions with *ARR5*, a marker gene of cytokinin pathway activation, and Mt *CRE1*, the main cytokinin receptor gene linked to nodulation, have revealed that the cytokinin pathway is active at later stages of the symbiotic interaction (Lohar et al., 2004, 2006). The expression of Mt *CRE1* is found in dividing cells of nodule primordium and is then restricted to the apical meristematic region of mature nodules. A reasonable assumption is therefore that cytokinins are required for nodule meristem activity. Cell differentiation in nodule zone II/III may involve a fine tuning of cytokinin action, with a gradient of decreasing cytokinin activity from the meristem to underlying tissues. We propose that EFD, which is maximally expressed at the border between zones I and II, participates in the control of this gradient by regulating the cytokinin pathway via the type-A response regulator Mt RR4. Altering this gradient in *efd-1* would lead to an enlarged zone II because the proximal zone II and zone III cannot form properly. Following this hypothesis, the nodule meristem would be reminiscent of shoot meristems more than of root meristems, cytokinins being thought in the latter to be required for cell differentiation rather than proliferation (Dello Ioio et al., 2007). EFD could thus be viewed as a factor that contributes to define spatially and temporally the niche for proliferating meristematic cells by turning down the cytokinin pathway. As documented for several key factors regulating development (Ferrell, 2002), the observed positive feedback regulation of EFD on its own expression is likely another important regulatory mechanism that allows *EFD* expression to be maintained in a defined region, thus leading to an irreversible developmental switch during nodule differentiation. The fact that *EFD* is also expressed in root meristems is intriguing, and further studies will be required to examine possible impacts of *EFD* on root development.

In conclusion, this study illustrates how high-throughput genomics tools set up for model legumes can contribute to the identification of novel and important regulators of nodule development. It is anticipated that a number of other regulators will be identified in the near future and characterized efficiently thanks to reverse genetics platforms. This will lead to the dissection of the developmental cascade controlling the formation of an organ that plays a central role for agricultural and environmental beneficial properties of legumes.

METHODS

Plant Growth and Bacterial Strains

Medicago truncatula cv Jemalong A17 was used as the wild-type reference and for backcrosses of the *efd-1* mutant. Surface-sterilized seeds were placed on inverted agar plates in the dark for 3 d at 8°C and 1 d at 20°C. Germinated seeds were transferred into pouches (cytologic studies), Farhaeus agar plates (treatments), or in aeroponic caissons (kinetic studies by Q-RT-PCR and backcross segregation analysis) containing an appropriate plant growth medium, as described in the *Medicago* handbook (http://www.noble.org/MedicagoHandbook/). Plants in pouches were inoculated with 600 μL of *Sinorhizobium meliloti* suspension at an OD_{600} = 0.02 and placed at 25°C (light-dark photoperiod: 16 h/8 h). Plant growth and inoculation in caisson were as described by Combier et al. (2007), with the following chamber conditions: temperature, 22°C; 75% hygrometry; light intensity, 200 $\mu E \cdot m^{-2} \cdot s^{-1}$; light-dark photoperiod, 16 h/8 h. For ACC and AVG treatments, plants were grown on Farhaeus medium in plates at 20°C with the same photoperiod.

Wild-type *S. meliloti* RCR2011 pXLGD4 (GMI6526) and *S. meliloti* RCR2011 *exoA* pXLGD4 (GMI3072) were grown at 28°C in tryptone yeast medium supplemented with 6 mM calcium chloride and 10 $\mu g\ mL^{-1}$ tetracycline. For root transformation, we used ARqua1 *Agrobacterium rhizogenes* as described by Boisson-Dernier et al. (2001). For *Nicotiana benthamiana* transient expression, we used *Agrobacterium tumefaciens* strains GV3101 and GV3103 (as in Andriankaja et al., 2007) grown at 28°C in Luria-Bertani medium supplemented with rifampicin (10 $\mu g\ mL^{-1}$).

ACC, AVG, NF, and Cytokinin Treatments

For ACC (Sigma-Aldrich) treatment, a 50 μM solution of ACC was applied onto roots of 5-d-old seedlings. Thirty roots per time point (0, 5, 24, and 48 h after treatment) were cut and frozen before RNA extraction. The impact of AVG (Sigma-Aldrich) treatment onto *EFD* induction was determined on *S. meliloti*–induced nodules from 50 independent roots. NF treatments (18 h for Q-RT-PCR, and until 48 h for *PEFD:GUS* observations) and root hairs isolation were done as described by Sauviac et al. (2005). Cytokinin (BAP; Sigma-Aldrich) treatments were done as described by Gonzalez-Rizzo et al. (2006), with or without a 1 h cycloheximide 100 μM treatment (Sigma-Aldrich). Three biological repetitions were done for each of these treatments.

Identification of the *efd-1* Deletion Mutant from a Fast Neutron Mutant Population

The *efd-1* deletion mutant was identified using De-TILLING (deletion TILLING), a novel reverse-genetics platform that has been established in

M. truncatula exploiting fast neutron mutagenesis and a highly sensitive PCR-based detection (C. Rogers and G. Oldroyd, unpublished data). A population of 60,000 M2 lines, prepared originally as 2400 DNA samples, was pooled to a set of 10 templates for PCR screening. The identification of false positives was avoided by simultaneously screening a differential pooling of these DNAs, giving a total of 20 PCR reactions. Genomic regions of 2 to 2.5 kb were identified possessing a unique restriction site adjacent to exon 1 of the *EFD* gene. Amplification of one of these genomic regions, a 2.55-kb target region centered on an *Eco*RI restriction site, revealed the presence of an ~1.5-kb deletion mutant within the population. This was confirmed by screening a second region of 2.9 kb centered on the same restriction site. Sequencing of these amplified fragments revealed a deletion covering nucleotides −656 to +915 (1571 bp), completely removing exon 1. Subsequent PCR screening of three-dimensional DNA pools allowed the mutant to be located and recovered from within archived M2 seed stocks.

The *EFD* genomic region was analyzed by PCR using the same primers as in Q-RT-PCR experiments (see Supplemental Table 7 online) and the two following primers: 5′-GGGGTACCCACCCCGAACCC-3′ and 5′-TGACCTTCAAACCCAACACA-3′.

Phenotypic Characterization of *efd-1*

S. meliloti spot inoculation was done as described by Mathis et al. (1999). Histological studies of nodules were performed after fixation in 2.5% of glutaraldehyde buffered in 0.1 M sodium phosphate buffer, pH 7.2, dehydration in an alcohol series, and embedding in Technovit 7100 resin (Hereaus Kulzer). Sections (4 μm thick) were observed after counterstaining in a 0.02% aqueous toluidine blue solution. For EM studies, following the glutaraldehyde fixation step, nodules were postfixed in 1% osmium phosphate buffer solution and embedded in epon as described by Vasse et al. (1993). Ultrathin sections stained with uranyl acetate and lead citrate were examined using a JEM 2100 electron microscope.

For mycorrhizal observations, germinating seeds of *efd-1* and A17 were placed on Farhaeus plates for 10 d and then transferred on M medium (Bécard and Fortin, 1988) plates (supplemented with 0.5% phytagel) with pouch paper and inoculated 9 d later by *Glomus intraradices* as described by Boisson-Dernier et al. (2005). Mycorrhizal coloration was done at 22 DAI with black ink (Sheaffer) as described by Chabaud et al. (2002).

Nitrogenase activity was assayed by the acetylene reduction technique (Hardy et al., 1968). Nitrogen fixation ability was measured on 10 individual wild-type or *efd-1* plants at 24 DAI. Data were calculated as a ratio between ethylene and acetylene peak heights given in percentage.

Plasmid Constructs and *A. rhizogenes* Transformation

To generate the *P*35S:*EFD:VP16* construct, we first introduced the *VP16* domain in the pPex vector (Combier et al., 2007). *VP16* was amplified on PFP101HAVP16 (from PZP200; Hajdukiewicz et al., 1994) with the primers 5′-AGGATCCCCAACGATGAAAAGCTTGGC-3′ and 5′-GATCC-GCTCTAGAGATATCC-3′ and introduced in pGEM-T (Promega) between *Bam*HI and *Xba*I sites. We amplified the *EFD* coding sequence using Pfx polymerase (Invitrogen) and primers 5′-ACTCGAGATGGCAAGACCA-CAACAACGTTATAG-3′ and 5′-AGGATCCAGATGAACCAACAGAACA-AAG-3′ and inserted it in pPex-VP16 between *Xho*I and *Bam*HI sites. To generate the *P35S*:*EFD* construct, we inserted the *Xho*I-*Bam*HI fragment from pPex-*EFD:VP16* plasmid into pPex between *Xho*I and *Bam*HI sites. Finally, we added into these two plasmids, at their *Kpn*I site, the *DsRED* gene from the pRed Root vector (Limpens et al., 2004).

For RNAi *EFD* construct, we used pPex-RNAi described by Combier et al. (2006). Using Pfx polymerase and primers 5′-TCAGTCCGCTC-GAGCCAAACAACAACAACCACCA-3′ and 5′-TTGGGAAGCTTAGAT-GAACCAACAGAACAAAG-3′ (sense cloning) and 5′-AAGGAAAAAAG-CGGCCGCCCAAACAACAACAACCACCA-3′ and 5′-CCTTTAAGACTA-GTAGATGAACCAACAGAACAAAG-3′ (antisense cloning), we amplified a 290-bp region of the *EFD* gene outside of the ERF domain that showed no similarity with other known *M. truncatula* genes. We cloned these fragments between *Xho*I and *Hin*dIII (sense) and *Not*I and *Spe*I (antisense) sites.

To generate the *PRR4:GUS* construct, we amplified an 1132-bp fragment from the CR962134.2 genomic BAC clone using Pfx polymerase and primers 5′-GGGGTACCCCCGAGAAAATAACT-3′ and 5′-CATGC-CATGGCACTCTCTTTGAAGAAAAAAAAGA-3′ and inserted it between *Kpn*I and *Nco*I sites of the pPex-GUS vector (Combier et al., 2007).

To generate the *PEFD:GUS* construct, since the *EFD* gene sequence was not available, we screened, using standard procedures, a 4.5× fraction of the *M. truncatula* mth2 BAC library (http://www.medicago.org/genome/) by hybridization on high-density filters. A 175-bp genomic *EFD* DNA fragment obtained by PCR amplification with primers 5′-CCAAA-CAACAACAACCACCA-3′ and 5′-TGACCTTCAAACCCAACACA-3′ was used as a probe and allowed to identify four BAC clones. We sequenced the mth2-4K7 BAC using primers listed in Supplemental Table 7 online. We then made two constructs with *PEFD*: the first one was based on a 1072-bp sequence amplified using Pfx polymerase and primers 5′-GGGGTACCCACCCCGAACCC-3′ and 5′-CATGCCATGGGATGAT-GAAACAAAAAAAAACGTG-3′ and inserted between *Kpn*I and *Nco*I sites of pPex-GUS; the second one was based on a 2.4-kb fragment, obtained by adding a 1375-bp sequence (from −1067 to −2441 of ATG) upstream of the first 1072-bp sequence, amplified by Pfx polymerase and primers 5′-GGGGTACCAATCATATTCGATGTGTATGAGAC-3′ and 5′-GGGGT-ACCTATATAACCGTTACC-3′ and inserted in *Kpn*I of the pPex-GUS containing the 1072-bp *PEFD* fragment.

The *efd-1* complementation construct was generated using *PEFD:GUS* constructs. The *GUS* gene was deleted by *Nco*I and *Not*I digestion and replaced by *EFD:Myc* from the overexpressing *EFD* construct in pPex.

All these constructs were checked by sequencing, introduced into *A. rhizogenes* strain ARqua1 by electroporation, and used for *M. truncatula* root transformation as described by Boisson-Dernier et al. (2001) and Combier et al. (2007). All *A. rhizogenes* root transformations were done in at least three biological repetitions, except for the *efd-1* complementation.

Plasmid Constructs and Transient Expression in *N. benthamiana*

The plasmid constructs were made in two steps. First, we cloned *EFD* and *EFD* deleted from the ERF domain (*ΔEFD*) in the gateway vector pKAs207 (kindly provided by L. Deslandes [LIPM, Toulouse] and corresponding to pDONR207 in which an *Asc*I kanamycin cassette has been introduced) and then we did an LR recombination with destination vectors PAM-PAT35S-GWY-mRFP/mRFP-GWY/GWY-3HA/3HA-GWY (provided by L. Deslandes) following the manufacturer's instructions (Invitrogen). For this step, we amplified the *EFD* coding sequence (588 bp) with or without the STOP codon, with Pfx polymerase and primers 5′-AGGCGCGCCTAC-CATGGCAAGACCACAACAACGTTAT-3′ and 5′-AGGCGCGCCCAGAT-GAACCAACAGAACAAAGCTC-3′ (within STOP codon) or 5′-AGGCGC-GCCCCTAAGATGAACCAACAGAACAAAG-3′ (without STOP codon). For *ΔEFD*, we amplified a 390-bp fragment using Pfx polymerase and primers 5′-AGGCGCGCCTACCATGCCAAATGGACCACAATCTTCT-TCA-3′ and 5′-AGGCGCGCCCAGATGAACCAACAGAACAAAGCTC-3′ (within STOP codon) or 5′-AGGCGCGCCCCTAAGATGAACCAACAGAA-CAAAG-3′ (without STOP codon).

For bacteria preparation and *N. benthamiana* infiltration, we used the protocol described by Andriankaja et al. (2007). The subcellular localization of mRFP-fused proteins was analyzed by fluorescence confocal microscopy (Leica AOBS SP2) from 30 to 72 h after infiltration. Each construct was observed in three independent infiltrated leaves and at least in three biological repetitions. Fluorescence was collected at 565 to 620 nm for mRFP and 630 to 730 nm for chloroplasts. For transactivation

studies, leaf discs were collected at 24 and 48 h after inoculation on independent infiltrated leaves using at least three biological repetitions. For each point, two discs were used directly for histochemical GUS assay and two were frozen in liquid nitrogen for enzymatic GUS assays on protein extracts.

Histochemical and Fluorometric GUS Assays

Histochemical GUS staining (using 5-bromo-4-chloro-3-indolyl-β-glucuronic acid; MP Biomedicals) and double staining for both GUS and β-galactosidase activities after inoculation with *S. meliloti* strain carrying a constitutive *hemA-lacZ* fusion (Ardourel et al., 1994) were performed as described by Boisson-Dernier et al. (2005). For simple β-galactosidase assays, we used X-Gal (5-bromo-4-chloro-3-indolyl-β-D-galactopyranoside; MP Biomedicals) instead of Magenta-Gal. Roots and nodule sections (50 μm thick) were prepared in 4% agarose with a vibrating microtome (Leica VT 1000S), and stained samples were observed with a Zeiss Axiophot light microscope. Observations were done at least on 10 independent roots transformed by *A. rhizogenes* and at least two biological repetitions, at different times after mock or *S. meliloti* inoculation.

For GUS quantitative assay, leaf discs of *N. benthamiana* were ground in liquid nitrogen and total proteins were extracted in GUS buffer (50 mM potassium phosphate buffer, pH 7.5, 10 mM 2-mercaptoethanol, 10 mM Na_2EDTA, 0.1% sodium lauryl-sarcosine, and 0.1% Triton X-100). Protein concentrations were normalized with Bradford reagent (Bio-Rad). Enzymatic reactions were performed using 10 μg of total protein extract with 4-methylumbelliferyl-β-D-glucuronide (Biosynth) as substrate. Fluorescence was measured using a microtiter fluorimeter (FL600; Bio-Tek) and measurements read every 30 min (during 4 h). Enzyme activity was calibrated with a dilution series of 4-methylumbelliferone (Sigma-Aldrich).

In Situ Hybridizations

In situ hybridizations were performed for *EFD* using a riboprobe made from the full-size cDNA as described by de Billy et al. (2001) on wild-type 4- and 10-d-old nodules harvested from plants grown in aeroponic caissons. For *Mt RR4*, in situ hybridizations were performed following the procedure described by Valoczi et al. (2006) and Boualem et al. (2008). The following primers were used for generating the Mt *RR4*–specific probe (251 nucleotides long): 5′-AATGTGGGAAGCCAAGACAC-3′ and 5′-CGGTGCCGGTCATTTAAG-3′. For the probe (182 nucleotides long) corresponding to the whole type-A response regulator gene family, the primers were 5′-ATGCTTTTGTTCCGGGTTTA-3′ and 5′-CGGTGCCGGTCATTTAAG-3′.

Q-RT-PCR Analysis

RNA samples were isolated using the SV total RNA extraction kit (Promega) according to the manufacturer's recommendations. The absence of DNA contamination was verified by PCR with *EF1-α* primers, and RNA quality was checked using a Bioanalyzer (Agilent Technologies). Reverse transcription was performed on 1 μg of RNA using the superscript reverse transcriptase II (Invitrogen) and anchored oligo(dT) for plant cDNAs synthesis and random hexamers for bacterial cDNAs. We used 80 pg per sample of human desmin RNA as external standard to check the efficiency of the reverse transcription and *EF1-α* (MtGI8: TC106470) or *pnp* (SMc00324) as internal Q-RT-PCR standard for the analysis of plant or bacterial gene expression, respectively. Quantitative PCR was performed on a Lightcycler (Roche Diagnostics), with the Light Cycler Fast Start Reaction Mix Master^{PLUS} SYBR Green according to the manufacturer's recommendations. Cycling conditions were as follow: 95°C for 8 min, 45 cycles at 95°C for 5 s, 60°C for 7 s, and 72°C for 15 s. The specificity of primer pairs (see Supplemental Table 8 online) was confirmed by sequencing PCR amplicon and analysis of dissociation curves (65 to 99°C). Each reaction was performed on a 1:16 (v/v) cDNA dilution with technical replicates. The data shown represent means of values obtained from two or three independent biological replicates.

Q-RT-PCR analysis was also conducted on 384-well plates for validation of microarray results using primers shown in Supplemental Table 8 online and an ABI 7900HT thermocycler (Applied Biosystems) following manufacturer conditions. Cycling conditions were as follow: 50°C for 2 min, 95°C for 10 min, 40 cycles at 95°C for 15 s, and 60°C for 1 min.

Microarray Studies

RNA was extracted from nodules by the Trizol method (Invitrogen) and purified using Microcon-30 column (Millipore). When analyzing *P35S:EFD:VP16* roots, RNA was prepared using the SV total RNA extraction kit (Promega) and amplified with the BD SMART mRNA amplification kit (BD Biosciences). Sixteen micrograms for the nodules and 5 μg for the root were used to synthesize Cy3- and Cy5-labeled cDNA (Hohnjec et al., 2005). Mt16kOLI1Plus microarrays (Hohnjec et al., 2005; Tellström et al., 2007) were used, the design of which can be viewed at http://www.ebi.ac.uk/arrayexpress (accession number A-MEXP-138). Three independent biological replicates were performed with a dye swap for each. Hybridization of targets, image acquisition, and analysis were performed precisely as described by Hohnjec et al. (2005), using an ASP hybridization station (Amersham Biosciences) and ImaGene 5.5 software (Biodiscovery).

Data files were processed using *EMMA2* array analysis software (Küster et al., 2007). Microarray data were normalized by Lowess normalization with a floor value of 20 and *t*-statistics used to identify differentially regulated genes. Adjusted P values were determined to carry out multiple-comparison corrections using the Benjamini and Hochberg method, which controls the false discovery rate (Benjamini and Hochberg, 1995; Reiner et al., 2003).

Phylogenetic Analysis of ERF Proteins

Full-length amino acid sequences of selected ERF proteins were aligned using ClustalW (http://clustalw.genome.ad.jp/) and analyzed with the PHYLIP software package (http://www.csc.fi/molbio/progs/phylip/doc/main.html). The tree was calculated on the basis of 1000 bootstraps and parsimony calculations using randomized inputs and 100× jumbling. The resulting 100 data sets were combined for a consensus tree. The resulting tree file was displayed using TreeView.

Accession Numbers

Sequence data for the proteins used for phylogenetic analyses can be found in the GenBank/EMBL data libraries under the following accession numbers: Mt ERN1, EU038802; Mt ERN2, EU038803; Mt ERN3, EU038804; At ERF002, At5g19790; At Rap2.11, NP_197480; At SHN1, At1g15360; At SHN2, At5g11190; At SHN3, At5g25390; At ERF003, At5g25190. Bacterial genes: *bacA*, SM-b20999; *nifH*, SMa0825; *nodF*, SMa0852; *pnp*, SMc00324. Mt *RR4* EST, TC103991 (MTGI8 database); Mt *ENOD11* gene, AJ297721. Results of gene expression profiling experiments are accessible at ArrayExpress under accession number E-TABM-393. The EFD name has priority (VandenBosch and Frugoli, 2001) and has been registered at the GenBank database (EU251063).

Supplemental Data

The following materials can be found in the online version of this article.

Supplemental Figure 1. Cortical Cell Divisions Are Frequently Associated with Root Hair Curls in the *efd-1* Mutant but Not in Wild-Type Plants.

Supplemental Figure 2. A Weak Supernodulant Phenotype Is Exhibited by *EFD* RNAi Roots.

Supplemental Figure 3. A Decrease in Nodulation Is Exhibited by *EFD*-Overexpressing Roots.

Supplemental Figure 4. Q-RT-PCR Analyses of Bacterial Symbiotic Gene Expression in *efd-1* versus Wild-Type Nodules.

Supplemental Figure 5. In Situ Hybridization on Nodule Sections with a Control ^{35}S-Labeled *EFD* Sense Probe.

Supplemental Figure 6. *EFD* Is Expressed in Root Tips and Root Primordia and Is Not Induced by Purified Nod Factors.

Supplemental Figure 7. *EFD* Expression Is Not Induced by Ethylene.

Supplemental Figure 8. Alignment of Group V ERF Proteins from *M. truncatula* and *Arabidopsis*.

Supplemental Figure 9. Mt *RR4* and *EFD* Are Expressed in Nodule Zone II.

Supplemental Figure 10. Mt *RR4* Is a Primary Cytokinin Response Gene, and *EFD* Transcription Is Not Regulated by Cytokinins.

Supplemental Figure 11. Trans-Activation of *PRR4*, *PEFD*, and *PMMPL1* in *N. benthamiana* by *P35S:EFD:HA*.

Supplemental Table 1. Q-RT-PCR Analysis of *EFD* Expression in Roots of Wild-Type and the *efd-1* Mutant of *M. truncatula* Inoculated by Wild-Type *S. meliloti*.

Supplemental Table 2. Infection Thread Formation Is Decreased in *EFD*-Overexpressing Roots.

Supplemental Table 3. Q-RT-PCR Analysis of *EFD* and Mt *ENOD11* Expression in Roots of Early Symbiotic *M. truncatula nfp-1* (C31 Allele), *nsp1-1* (B85), and *hcl-1* (B56) Mutants Inoculated by Wild-Type *S. meliloti*.

Supplemental Table 4. Genes Differentially Expressed between Wild-Type and *efd-1* Nodules as Determined by Microarray Analyses.

Supplemental Table 5. Q-RT-PCR Validation of Genes Identified by Mt16KOLI1Plus Microarrays as Down- or Upregulated in *efd-1* Nodules Compared with Wild-Type Nodules.

Supplemental Table 6. Genes Differentially Expressed between *P35S:EFD* Transgenic *M. truncatula* Roots and Empty Vector Transformed Roots, with (4 DAI) and without *S. meliloti* Inoculation, as Determined by Microarray Analyses.

Supplemental Table 7. Primers Used for *PEFD* Sequencing.

Supplemental Table 8. Primers Used in Q-RT-PCR.

ACKNOWLEDGMENTS

We thank Helge Küster (Bielefeld University, Germany) for providing 16K+ microarrays and accompanying procedures and Jérôme Gouzy for complementary information on gene annotation. We also thank Delphine Capela (Laboratoire des Interactions Plantes Micro-Organismes [LIPM]), Frédéric Debéllé (LIPM), Laurent Deslandes (LIPM), Alain Jauneau (IFR40, Toulouse), and Thomas Ott (LIPM) for their help with acetylene reduction assay, cloning vectors, BAC library screening, confocal microscopy, and phylogenetic analyses, respectively. We are grateful to Martin Crespi (Institut des Sciences du Végétal) and Jean Dénarié (LIPM, Toulouse) for useful comments on the manuscript and to Fernanda de Carvalho Niebel (LIPM) for fruitful discussions and sharing unpublished data. We wish to acknowledge the contribution of José Garcia (LIPM) for plant production and Christelle Latorre (LIPM) for some Q-RT-PCR analyses. *M. truncatula* wild-type A17 seeds were provided by Jean-Marie Prospéri (Institut National de la Recherche Agronomique). This work was supported by the FP6 Grain Legumes Integrated Project. Tatiana Vernié and Julie Plet were supported by a doctoral grant from EU-CNRS (fonds social européen) and from the French Research Ministry, respectively.

Received April 5, 2008; revised September 22, 2008; accepted October 16, 2008; published October 31, 2008.

REFERENCES

Aharoni, A., Dixit, S., Jetter, R., Thoenes, E., van Arkel, G., and Pereira, A. (2004). The SHINE clade of AP2 domain transcription factors activates wax biosynthesis, alters cuticle properties, and confers drought tolerance when overexpressed in Arabidopsis. Plant Cell **16:** 2463–2480.

Allen, M.D., Yamasaki, K., Ohme-Takagi, M., Tateno, M., and Suzuki, M. (1998). A novel mode of DNA recognition by a beta-sheet revealed by the solution structure of the GCC-box binding domain in complex with DNA. EMBO J. **17:** 5484–5496.

Alunni, B., Kevei, Z., Redondo-Nieto, M., Kondorosi, A., Mergaert, P., and Kondorosi, E. (2007). Genomic organization and evolutionary insights on GRP and NCR genes, two large nodule-specific gene families in *Medicago truncatula.* Mol. Plant Microbe Interact. **20:** 1138–1148.

Andriankaja, A., Boisson-Dernier, A., Frances, L., Sauviac, L., Jauneau, A., Barker, D.G., and de Carvalho-Niebel, F. (2007). AP2-ERF transcription factors mediate Nod factor dependent Mt *ENOD11* activation in root hairs via a novel cis-regulatory motif. Plant Cell **19:** 2866–2885.

Ardourel, M., Demont, N., Debelle, F., Maillet, F., de Billy, F., Prome, J.C., Denarie, J., and Truchet, G. (1994). *Rhizobium meliloti* lipooligosaccharide nodulation factors: Different structural requirements for bacterial entry into target root hair cells and induction of plant symbiotic developmental responses. Plant Cell **6:** 1357–1374.

Arrighi, J.F., Godfroy, O., de Billy, F., Saurat, O., Jauneau, A., and Gough, C. (2008). The RPG gene of *Medicago truncatula* controls Rhizobium-directed polar growth during infection. Proc. Natl. Acad. Sci. USA **105:** 9817–9822.

Asamizu, E., Shimoda, Y., Kouchi, H., Tabata, S., and Sato, S. (2008). A positive regulatory role for *LjERF1* in the nodulation process is revealed by systematic analysis of nodule-associated transcription factors of *Lotus japonicus.* Plant Physiol. **147:** 2030–2040.

Banno, H., Ikeda, Y., Niu, Q.W., and Chua, N.H. (2001). Overexpression of Arabidopsis ESR1 induces initiation of shoot regeneration. Plant Cell **13:** 2609–2618.

Bécard, G., and Fortin, J.A. (1988). Early events of vesicular-arbuscular mycorrhiza formation on Ri T-DNA transformed roots. New Phytol. **108:** 211–218.

Becker, A., et al. (2004). Global changes in gene expression in *Sinorhizobium meliloti* 1021 under microoxic and symbiotic conditions. Mol. Plant Microbe Interact. **17:** 292–303.

Benaben, V., Duc, G., Lefebvre, V., and Huguet, T. (1995). TE7, an inefficient symbiotic mutant of *Medicago truncatula* Gaertn. cv Jemalong. Plant Physiol. **107:** 53–62.

Benjamini, Y., and Hochberg, Y. (1995). Controlling the false discovery rate: a practical and powerful approch to multiple testing. J. Roy. Statist. Soc. Ser. B. Methodological **57:** 289–300.

Boisson-Dernier, A., Andriankaja, A., Chabaud, M., Niebel, A., Journet, E.P., Barker, D.G., and de Carvalho-Niebel, F. (2005). *MtENOD11* gene activation during rhizobial infection and mycorrhizal

arbuscule development requires a common AT-rich-containing regulatory sequence. Mol. Plant Microbe Interact. **18:** 1269–1276.

Boisson-Dernier, A., Chabaud, M., Garcia, F., Becard, G., Rosenberg, C., and Barker, D.G. (2001). *Agrobacterium rhizogenes*-transformed roots of *Medicago truncatula* for the study of nitrogen-fixing and endomycorrhizal symbiotic associations. Mol. Plant Microbe Interact. **14:** 695–700.

Borisov, A.Y., Madsen, L.H., Tsyganov, V.E., Umehara, Y., Voroshilova, V.A., Batagov, A.O., Sandal, N., Mortensen, A., Schauser, L., Ellis, N., Tikhonovich, I.A., and Stougaard, J. (2003). The *Sym35* gene required for root nodule development in pea is an ortholog of *Nin* from *Lotus japonicus.* Plant Physiol. **131:** 1009–1017.

Boualem, A., Laporte, P., Jovanovic, M., Laffont, C., Plet, J., Combier, J.P., Niebel, A., Crespi, M., and Frugier, F. (2008). MicroRNA166 controls root and nodule development in *Medicago truncatula.* Plant J. **54:** 876–887.

Boutilier, K., Offringa, R., Sharma, V.K., Kieft, H., Ouellet, T., Zhang, L., Hattori, J., Liu, C.M., van Lammeren, A.A., Miki, B.L., Custers, J.B., and van Lookeren Campagne, M.M. (2002). Ectopic expression of BABY BOOM triggers a conversion from vegetative to embryonic growth. Plant Cell **14:** 1737–1749.

Bright, L.J., Liang, Y., Mitchell, D.M., and Harris, J.M. (2005). The *LATD* gene of *Medicago truncatula* is required for both nodule and root development. Mol. Plant Microbe Interact. **18:** 521–532.

Chabaud, M., Venard, D., Defaux-Petras, A., Bécard, G., and Barker, D.G. (2002). Targeted inoculation of *Medicago truncatula* in vitro root cultures reveals *MtENOD11* expression during early stages of infection by arbuscular mycorrhizal fungi. New Phytol. **156:** 265–273.

Chuck, G., Muszynski, M., Kellogg, E., Hake, S., and Schmidt, R.J. (2002). The control of spikelet meristem identity by the branched *silkless1* gene in maize. Science **298:** 1238–1241.

Combier, J.P., de Billy, F., Gamas, P., Niebel, A., and Rivas, S. (2008). Trans-regulation of the expression of the transcription factor MtHAP2–1 by a uORF controls root nodule development. Genes Dev. **22:** 1549–1559.

Combier, J.P., Frugier, F., de Billy, F., Boualem, A., El-Yahyaoui, F., Moreau, S., Vernie, T., Ott, T., Gamas, P., Crespi, M., and Niebel, A. (2006). MtHAP2-1 is a key transcriptional regulator of symbiotic nodule development regulated by microRNA169 in *Medicago truncatula.* Genes Dev. **20:** 3084–3088.

Combier, J.P., Vernié, T., de Billy, F., El Yahyaoui, F., Mathis, R., and Gamas, P. (2007). The MtMMPL1 early nodulin is a novel member of the matrix metalloendoproteinase family with a role in *Medicago truncatula* infection by *Sinorhizobium meliloti.* Plant Physiol. **144:** 703–716.

Cumming, G., Fidler, F., and Vaux, D.L. (2007). Errors bars in experimental biology. J. Cell Biol. **177:** 7–11.

de Billy, F., Grosjean, C., May, S., Bennett, M., and Cullimore, J.V. (2001). Expression studies on AUX1-like genes in *Medicago truncatula* suggest that auxin is required at two steps in early nodule development. Mol. Plant Microbe Interact. **14:** 267–277.

Dello Ioio, R., Linhares, F.S., Scacchi, E., Casamitjana-Martinez, E., Heidstra, R., Costantino, P., and Sabatini, S. (2007). Cytokinins determine Arabidopsis root-meristem size by controlling cell differentiation. Curr. Biol. **17:** 678–682.

Doerner, P. (2007). Plant meristems: Cytokinins–the alpha and omega of the meristem. Curr. Biol. **17:** R321–R323.

El Yahyaoui, F., Küster, H., Ben Amor, B., Hohnjec, N., Puhler, A., Becker, A., Gouzy, J., Vernie, T., Gough, C., Niebel, A., Godiard, L., and Gamas, P. (2004). Expression profiling in *Medicago truncatula* identifies more than 750 genes differentially expressed during nodulation, including many potential regulators of the symbiotic program. Plant Physiol. **136:** 3159–3176.

Fedorova, M., van de Mortel, J., Matsumoto, P.A., Cho, J., Town, C.D., VandenBosch, K.A., Gantt, J.S., and Vance, C.P. (2002). Genome-wide identification of nodule-specific transcripts in the model legume *Medicago truncatula.* Plant Physiol. **130:** 519–537.

Ferguson, B.J., and Mathesius, U. (2003). Signaling interactions during nodule development. J. Plant Growth Regul. **22:** 47–72.

Ferreira, F.J., and Kieber, J.J. (2005). Cytokinin signaling. Curr. Opin. Plant Biol. **8:** 518–525.

Ferrell, J.E., Jr. (2002). Self-perpetuating states in signal transduction: positive feedback, double-negative feedback and bistability. Curr. Opin. Cell Biol. **14:** 140–148.

Frugier, F., Kosuta, S., Murray, J.D., Crespi, M., and Szczyglowski, K. (2008). Cytokinin: Secret agent of symbiosis. Trends Plant Sci. **13:** 115–120.

Frugier, F., Poirier, S., Satiat-Jeunemaitre, B., Kondorosi, A., and Crespi, M. (2000). A Kruppel-like zinc finger protein is involved in nitrogen-fixing root nodule organogenesis. Genes Dev. **14:** 475–482.

Glazebrook, J., Ichige, A., and Walker, G.C. (1993). A *Rhizobium meliloti* homolog of the *Escherichia coli* peptide-antibiotic transport protein SbmA is essential for bacteroid development. Genes Dev. **7:** 1485–1497.

Godiard, L., Niebel, A., Micheli, F., Gouzy, J., Ott, T., and Gamas, P. (2007). Identification of new potential regulators of the *Medicago truncatula-Sinorhizobium meliloti* symbiosis using a large-scale suppression subtractive hybridization approach. Mol. Plant Microbe Interact. **20:** 321–332.

Gonzalez-Rizzo, S., Crespi, M., and Frugier, F. (2006). The *Medicago truncatula* CRE1 cytokinin receptor regulates lateral root development and early symbiotic interaction with *Sinorhizobium meliloti.* Plant Cell **18:** 2680–2693.

Graham, M.A., Silverstein, K.A., Cannon, S.B., and VandenBosch, K.A. (2004). Computational identification and characterization of novel genes from legumes. Plant Physiol. **135:** 1179–1197.

Guo, H., and Ecker, J.R. (2004). The ethylene signaling pathway: New insights. Curr. Opin. Plant Biol. **7:** 40–49.

Gutterson, N., and Reuber, T.L. (2004). Regulation of disease resistance pathways by AP2/ERF transcription factors. Curr. Opin. Plant Biol. **7:** 465–471.

Hajdukiewicz, P., Svab, Z., and Maliga, P. (1994). The small, versatile pPZP family of Agrobacterium binary vectors for plant transformation. Plant Mol. Biol. **25:** 989–994.

Hardy, R.W., Holsten, R.D., Jackson, E.K., and Burns, R.C. (1968). The acetylene-ethylene assay for N(2) fixation: Laboratory and field evaluation. Plant Physiol. **43:** 1185–1207.

Heckmann, A.B., Lombardo, F., Miwa, H., Perry, J.A., Bunnewell, S., Parniske, M., Wang, T.L., and Downie, J.A. (2006). *Lotus japonicus* nodulation requires two GRAS domain regulators, one of which is functionally conserved in a non-legume. Plant Physiol. **142:** 1739–1750.

Hohnjec, N., Vieweg, M.F., Puhler, A., Becker, A., and Küster, H. (2005). Overlaps in the transcriptional profiles of *Medicago truncatula* roots inoculated with two different Glomus fungi provide insights into the genetic program activated during arbuscular mycorrhiza. Plant Physiol. **137:** 1283–1301.

Jones, K.M., Kobayashi, H., Davies, B.W., Taga, M.E., and Walker, G.C. (2007). How rhizobial symbionts invade plants: the *Sinorhizobium-Medicago* model. Nat. Rev. Microbiol. **5:** 619–633.

Kalo, P., et al. (2005). Nodulation signaling in legumes requires NSP2, a member of the GRAS family of transcriptional regulators. Science **308:** 1786–1789.

Kawaguchi, M., Imaizumi-Anraku, H., Koiwa, H., Niwa, S., Ikuta, A., Syono, K., and Akao, S. (2002). Root, root hair, and symbiotic mutants of the model legume *Lotus japonicus.* Mol. Plant Microbe Interact. **15:** 17–26.

Kirch, T., Simon, R., Grunewald, M., and Werr, W. (2003). The *DORNROSCHEN/ENHANCER OF SHOOT REGENERATION1* gene of Arabidopsis acts in the control of meristem cell fate and lateral organ development. Plant Cell **15:** 694–705.

Krusell, L., et al. (2005). The sulfate transporter SST1 is crucial for symbiotic nitrogen fixation in *Lotus japonicus* root nodules. Plant Cell **17:** 1625–1636.

Krusell, L., et al. (2002). Shoot control of root development and nodulation is mediated by a receptor-like kinase. Nature **420:** 422–426.

Kumagai, H., Hakoyama, T., Umehara, Y., Sato, S., Kaneko, T., Tabata, S., and Kouchi, H. (2007). A novel ankyrin-repeat membrane protein, IGN1, is required for persistence of nitrogen-fixing symbiosis in root nodules of *Lotus japonicus.* Plant Physiol. **143:** 1293–1305.

Kuppusamy, K.T., Endre, G., Prabhu, R., Penmetsa, R.V., Veereshlingam, H., Cook, D.R., Dickstein, R., and Vandenbosch, K.A. (2004). *LIN*, a *Medicago truncatula* gene required for nodule differentiation and persistence of rhizobial infections. Plant Physiol. **136:** 3682–3691.

Küster, H., et al. (2007). Development of bioinformatic tools to support EST-sequencing, in silico- and microarray-based transcriptome profiling in mycorrhizal symbioses. Phytochemistry **68:** 19–32.

Limpens, E., Mirabella, R., Fedorova, E., Franken, C., Franssen, H., Bisseling, T., and Geurts, R. (2005). Formation of organelle-like N2-fixing symbiosomes in legume root nodules is controlled by DMI2. Proc. Natl. Acad. Sci. USA **102:** 10375–10380.

Limpens, E., Ramos, J., Franken, C., Raz, V., Compaan, B., Franssen, H., Bisseling, T., and Geurts, R. (2004). RNA interference in *Agrobacterium rhizogenes*-transformed roots of Arabidopsis and *Medicago truncatula.* J. Exp. Bot. **55:** 983–992.

Lohar, D.P., Schaff, J.E., Laskey, J.G., Kieber, J.J., Bilyeu, K.D., and Bird, D.M. (2004). Cytokinins play opposite roles in lateral root formation, and nematode and Rhizobial symbioses. Plant J. **38:** 203–214.

Lohar, D.P., Sharopova, N., Endre, G., Penuela, S., Samac, D., Town, C., Silverstein, K.A., and VandenBosch, K.A. (2006). Transcript analysis of early nodulation events in *Medicago truncatula.* Plant Physiol. **140:** 221–234.

Marsh, J.F., Rakocevic, A., Mitra, R.M., Brocard, L., Sun, J., Eschstruth, A., Long, S.R., Schultze, M., Ratet, P., and Oldroyd, G.E. (2007). *Medicago truncatula* NIN is essential for rhizobial-independent nodule organogenesis induced by autoactive calcium/calmodulin-dependent protein kinase. Plant Physiol. **144:** 324–335.

Marsch-Martinez, N., Greco, R., Becker, J.D., Dixit, S., Bergervoet, J.H., Karaba, A., de Folter, S., and Pereira, A. (2006). BOLITA, an Arabidopsis AP2/ERF-like transcription factor that affects cell expansion and proliferation/differentiation pathways. Plant Mol. Biol. **62:** 825–843.

Mathis, R., Grosjean, C., de Billy, F., Huguet, T., and Gamas, P. (1999). The early nodulin gene *MtN6* is a novel marker for events preceding infection of *Medicago truncatula* roots by *Sinorhizobium meliloti.* Mol. Plant Microbe Interact. **12:** 544–555.

Mergaert, P., Nikovics, K., Kelemen, Z., Maunoury, N., Vaubert, D., Kondorosi, A., and Kondorosi, E. (2003). A novel family in *Medicago truncatula* consisting of more than 300 nodule-specific genes coding for small, secreted polypeptides with conserved cysteine motifs. Plant Physiol. **132:** 161–173.

Mergaert, P., Uchiumi, T., Alunni, B., Evanno, G., Cheron, A., Catrice, O., Mausset, A.E., Barloy-Hubler, F., Galibert, F., Kondorosi, A., and Kondorosi, E. (2006). Eukaryotic control on bacterial cell cycle and differentiation in the Rhizobium-legume symbiosis. Proc. Natl. Acad. Sci. USA **103:** 5230–5235.

Middleton, P.H., et al. (2007). An ERF transcription factor in *Medicago truncatula* that is essential for Nod factor signal transduction. Plant Cell **19:** 1221–1234.

Morandi, D., Prado, E., Sagan, M., and Duc, G. (2005). Characterisation of new symbiotic *Medicago truncatula* (Gaertn.) mutants, and phenotypic or genotypic complementary information on previously described mutants. Mycorrhiza **15:** 283–289.

Murray, J.D., Karas, B.J., Sato, S., Tabata, S., Amyot, L., and Szczyglowski, K. (2007). A cytokinin perception mutant colonized by Rhizobium in the absence of nodule organogenesis. Science **315:** 101–104.

Naito, Y., Fujie, M., Usami, S., Murooka, Y., and Yamada, T. (2000). The involvement of a cysteine proteinase in the nodule development in Chinese milk vetch infected with *Mesorhizobium huakuii* subsp. *renge*i. Plant Physiol. **124:** 1087–1096.

Nakano, T., Suzuki, K., Fujimura, T., and Shinshi, H. (2006). Genome-wide analysis of the ERF gene family in Arabidopsis and rice. Plant Physiol. **140:** 411–432.

Naya, L., Ladrera, R., Ramos, J., Gonzales, E.M., Arrese-Igor, C., Minchin, F.R., and Becana, M. (2007). The response of carbon metabolism and antioxidant defenses of alfalfa nodules to drought stress and to the subsequent recovery of plants. Plant Physiol. **144:** 1104–1114.

Nishimura, R., Hayashi, M., Wu, G.J., Kouchi, H., Imaizumi-Anraku, H., Murakami, Y., Kawasaki, S., Akao, S., Ohmori, M., Nagasawa, M., Harada, K., and Kawaguchi, M. (2002b). HAR1 mediates systemic regulation of symbiotic organ development. Nature **420:** 426–429.

Nishimura, R., Ohmori, M., Fujita, H., and Kawaguchi, M. (2002a). A Lotus basic leucine zipper protein with a RING-finger motif negatively regulates the developmental program of nodulation. Proc. Natl. Acad. Sci. USA **99:** 15206–15210.

Noh, Y.S., and Amasino, R.M. (1999). Identification of a promoter region responsible for the senescence-specific expression of *SAG12.* Plant Mol. Biol. **41:** 181–194.

Nukui, N., Ezura, H., and Minamisawa, K. (2004). Transgenic *Lotus japonicus* with an ethylene receptor gene *Cm-ERS1/H70A* enhances formation of infection threads and nodule primodia. Plant Cell Physiol. **45:** 427–435.

Oka-Kira, E., and Kawaguchi, M. (2006). Long-distance signaling to control root nodule number. Curr. Opin. Plant Biol. **9:** 496–502.

Oldroyd, G.E., and Downie, J.A. (2006). Nuclear calcium changes at the core of symbiosis signalling. Curr. Opin. Plant Biol. **9:** 351–357.

Oldroyd, G.E., and Downie, J.A. (2008). Coordinating nodule morphogenesis with rhizobial infection in legumes. Annu. Rev. Plant Biol. **59:** 519–546.

Oldroyd, G.E., and Long, S.R. (2003). Identification and characterization of nodulation-signaling pathway 2, a gene of *Medicago truncatula* involved in Nod factor signaling. Plant Physiol. **131:** 1027–1032.

Penmetsa, R.V., and Cook, D.R. (1997). A legume ethylene-insensitive mutant hyperinfected by its rhizobial symbiont. Science **275:** 527–530.

Pislariu, C.I., and Dickstein, R. (2007). An IRE-like AGC kinase gene, *MtIRE*, has unique expression in the invasion zone of developing root nodules in *Medicago truncatula.* Plant Physiol. **144:** 682–694.

Reiner, A., Yekutieli, D., and Benjamini, Y. (2003). Identifying differentially expressed genes using false discovery rate controlling procedures. Bioinformatics **19:** 368–375.

Riechmann, J.L., and Meyerowitz, E.M. (1998). The AP2/EREBP family of plant transcription factors. Biol. Chem. **379:** 633–646.

Sauviac, L., Niebel, A., Boisson-Dernier, A., Barker, D.G., and de Carvalho-Niebel, F. (2005). Transcript enrichment of Nod factor-elicited early nodulin genes in purified root hair fractions of the model legume *Medicago truncatula.* J. Exp. Bot. **56:** 2507–2513.

Schauser, L., Handberg, K., Sandal, N., Stiller, J., Thykjaer, T.,

Pajuelo, E., Nielsen, A., and Stougaard, J. (1998). Symbiotic mutants deficient in nodule establishment identified after T-DNA transformation of *Lotus japonicus.* Mol. Gen. Genet. **259:** 414–423.

Schnabel, E., Journet, E.P., de Carvalho-Niebel, F., Duc, G., and Frugoli, J. (2005). The *Medicago truncatula SUNN* gene encodes a CLV1-like leucine-rich repeat receptor kinase that regulates nodule number and root length. Plant Mol. Biol. **58:** 809–822.

Schauser, L., Roussis, A., Stiller, J., and Stougaard, J. (1999). A plant regulator controlling development of symbiotic root nodules. Nature **402:** 191–195.

Searle, I.R., Men, A.E., Laniya, T.S., Buzas, D.M., Iturbe-Ormaetxe, I., Carroll, B.J., and Gresshoff, P.M. (2003). Long-distance signaling in nodulation directed by a CLAVATA1-like receptor kinase. Science **299:** 109–112.

Silverstein, K.A., Graham, M.A., and VandenBosch, K.A. (2006). Novel paralogous gene families with potential function in legume nodules and seeds. Curr. Opin. Plant Biol. **9:** 142–146.

Silverstein, K.A., Moskal, W.A., Jr., Wu, H.C., Underwood, B.A., Graham, M.A., Town, C.D., and VandenBosch, K.A. (2007). Small cysteine-rich peptides resembling antimicrobial peptides have been under-predicted in plants. Plant J. **51:** 262–280.

Smit, P., Raedts, J., Portyanko, V., Debelle, F., Gough, C., Bisseling, T., and Geurts, R. (2005). NSP1 of the GRAS protein family is essential for rhizobial Nod factor-induced transcription. Science **308:** 1789–1791.

Starker, C.G., Parra-Colmenares, A.L., Smith, L., Mitra, R.M., and Long, S.R. (2006). Nitrogen fixation mutants of *Medicago truncatula* fail to support plant and bacterial symbiotic gene expression. Plant Physiol. **140:** 671–680.

Szczyglowski, K., Shaw, R., Wopereis, J., Copeland, S., Hamburger, D., Kasiborski, B., Dazzo, F.B., and de Bruijn, F. (1998). Nodule organogenesis and symbiotic mutants of the model legume *Lotus japonicus.* Mol. Plant Microbe Interact. **7:** 684–697.

Teillet, A., Garcia, J., de Billy, F., Gherardi, M., Huguet, T., Barker, D.G., de Carvalho-Niebel, F., and Journet, E.P. (2008). *api*, a novel *Medicago truncatula* symbiotic mutant impaired in nodule primordium invasion. Mol. Plant Microbe Interact. **21:** 535–546.

Tellström, V., Usadel, B., Thimm, O., Stitt, M., Küster, H., and Niehaus, K. (2007). The lipopolysaccharide of *Sinorhizobium meliloti* suppresses defense-associated gene expression in cell cultures of the host plant *Medicago truncatula.* Plant Physiol. **143:** 825–837.

Timmers, A.C., Auriac, M.C., and Truchet, G. (1999). Refined analysis of early symbiotic steps of the Rhizobium-Medicago interaction in relationship with microtubular cytoskeleton rearrangements. Development **126:** 3617–3628.

Tirichine, L., Sandal, N., Madsen, L.H., Radutoiu, S., Albrektsen, A.S., Sato, S., Asamizu, E., Tabata, S., and Stougaard, J. (2007). A gain-of-function mutation in a cytokinin receptor triggers spontaneous root nodule organogenesis. Science **315:** 104–107.

To, J.P., Haberer, G., Ferreira, F.J., Deruere, J., Mason, M.G., Schaller, G.E., Alonso, J.M., Ecker, J.R., and Kieber, J.J. (2004). Type-A Arabidopsis response regulators are partially redundant negative regulators of cytokinin signaling. Plant Cell **16:** 658–671.

Valoczi, A., Varallyay, E., Kauppinen, S., Burgyan, J., and Havelda, Z. (2006). Spatio-temporal accumulation of microRNAs is highly coordinated in developing plant tissues. Plant J. **47:** 140–151.

VandenBosch, K.A., and Frugoli, J. (2001). Guidelines for genetic nomenclature and community governance for the model legume *Medicago truncatula.* Mol. Plant Microbe Interact. **14:** 1364–1367.

van der Graaff, E., Dulk-Ras, A.D., Hooykaas, P.J., and Keller, B. (2000). Activation tagging of the *LEAFY PETIOLE* gene affects leaf petiole development in *Arabidopsis thaliana.* Development **127:** 4971–4980.

Van de Velde, W., Guerra, J.C., De Keyser, A., De Rycke, R., Rombauts, S., Maunoury, N., Mergaert, P., Kondorosi, E., Holsters, M., and Goormachtig, S. (2006). Aging in legume symbiosis. A molecular view on nodule senescence in *Medicago truncatula.* Plant Physiol. **141:** 711–720.

Vasse, J., de Billy, F., Camut, S., and Truchet, G. (1990). Correlation between ultrastructural differentiation of bacteroids and nitrogen fixation in alfalfa nodules. J. Bacteriol. **172:** 4295–4306.

Vasse, J., de Billy, F., and Truchet, G. (1993). Abortion of infection during the *Rhizobium meliloti*-alfalfa symbiotic interaction is accompanied by a hypersensitive reaction. Plant J. **4:** 555–566.

Veereshlingam, H., Haynes, J.G., Penmetsa, R.V., Cook, D.R., Sherrier, D.J., and Dickstein, R. (2004). *nip*, a symbiotic *Medicago truncatula* mutant that forms root nodules with aberrant infection threads and plant defense-like response. Plant Physiol. **136:** 3692–3702.

Wilde, R.J., Cooke, S.E., Brammar, W.J., and Schuch, W. (1994). Control of gene expression in plant cells using a 434:VP16 chimeric protein. Plant Mol. Biol. **24:** 381–388.

Wilson, K., Long, D., Swinburne, J., and Coupland, G. (1996). A Dissociation insertion causes a semidominant mutation that increases expression of *TINY*, an Arabidopsis gene related to *APETALA2.* Plant Cell **8:** 659–671.

Yang, W.C., de Blank, C., Meskiene, I., Hirt, H., Bakker, J., van Kammen, A., Franssen, H., and Bisseling, T. (1994). Rhizobium nod factors reactivate the cell cycle during infection and nodule primordium formation, but the cycle is only completed in primordium formation. Plant Cell **6:** 1415–1426.